SUPPORTING INFORMATION FOR ADDITION AND CORRECTION

An Organic White Light-Emitting Fluorophore

Youjun Yang, Mark Lowry, Corin M. Schowalter, Sayo O. Fakayode, Jorge O. Escobedo,*

Xiangyang Xu, Huating Zhang, Timothy J. Jensen, Frank R. Fronczek,

Isiah M. Warner and Robert M. Strongin**

Department of Chemistry, Louisiana State University, Baton Rouge, LA 70803

rstrong@lsu.edu

Page #	Content
Page S2	Introduction to the additions and corrections contained in the supporting information.
Page S5	Scheme S1 and experimental procedures for new synthesis of compound **17**, **SNAFR-1** and **SNAFR-2.**
Page S7	Figure S1, overlay of the ^{1}H NMR of **SNAFR-1**, **SNAFR-2** and the previously published **SNAFR-1** and **SNAFR-2** mixture.
	Figure S2, 2D COSY NMRs of **SNAFR-1** and **SNAFR-2.**
Page S8	Figure S3, Ortep drawing of **SNAFR-2.**
	Scheme S2, Formation of **SNAFR-1** MeOH and MeOH-d_4 adducts.
	Figure S4, Overlay of ^{1}H NMR of **SNAFR-1** MeOH and MeOH-d_4 (**18** and **19**) adducts
Page S9	Figure S5, EEMs of **SNAFR-1** MeOH adduct (Compound **18)** in DMSO and MeOH.
	Figure S6, EEM of **SNAFR-1** in DMSO and an expansion of the NIR emission.
	Figure S7, EEMs of **SNAFR-2** in MeOH and DMSO.
Page S10	Figure S8, EEM, emission when excited at 300 nm, and chromaticity diagram of **SNAFR-2** in DMSO with 0.25% 50 mM phosphate buffer at pH 7.5.
	Figure S9, Titration **SNAFR-2** in DMSO with 0.25% phosphate buffer.
Page S11	Scheme S3, Formation of **SNAFR-2** MeOH adduct via prior activation.
	Figure S10, EEM and chromaticity diagram of **SNAFR-2** in DMSO after addition of HCl, MeOH and phosphate buffer.
	Figure S11, Titration of **SNAFR-2** in 50 mM phosphate buffer with 0.25% DMSO.
Page S13	Figure S12, ^{1}H NMR of Compound **17** in DMSO-d_6.
Page S14	Figure S13, ^{13}C NMR of Compound **17** in DMSO-d_6.
Page S15	Figure S14, 2D COSY NMR of Compound **17** in DMSO-d_6.

Page S16	Figure S15, MALDI-TOF MS of Compound **17**.
Page S17	Figure S16, HPLC trace of Compound **17**.
Page S18	Figure S17, ^{1}H NMR of **SNAFR-1** in DMSO- d_6.
Page S19	Figure S18, ^{13}C NMR of **SNAFR-1** in DMSO- d_6.
Page S20	Figure S19, 2D COSY NMR of **SNAFR-1** in DMSO- d_6.
Page S21	Figure S20, MALDI-TOF MS of **SNAFR-1**.
Page S22	Figure S21, HPLC trace of **SNAFR-1**.
Page S23	Figure S22, ^{1}H NMR of **SNAFR-2** in DMSO- d_6.
Page S24	Figure S23, ^{13}C NMR of **SNAFR-2** in DMSO- d_6.
Page S25	Figure S24, 2D COSY NMR of **SNAFR-2** in DMSO- d_6.
Page S26	Figure S25, MALDI-TOF MS of **SNAFR-2**.
Page S27	Figure S26, HPLC trace of **SNAFR-2**.
Page S28	Figure S27, 2D COSY NMR of compound **12**.
Page S29	Figure S28, 2D ROESY NMR of compound **12**.
Page S30	Figure S29, HPLC trace of compound **12**.
Page S31	Figure S30, ^{1}H NMR of compound **18** in DMSO- d_6.
Page S32	Figure S31, ^{1}H NMR of compound **19** in DMSO- d_6.
Page S33	Figure S32, 2D COSY NMR of compound **19** in MeOH-d_4.
Page S34	Figure S33, ^{1}H NMR of the **SNAFR-1** H_2O adduct in DMSO- d_6.
Page S35	Figure S34, 2D COSY of the **SNAFR-1** H_2O adduct in DMSO- d_6.
Page S36	Table S1, Assignment of the protons of compound **17** via a 2D COSY.
	Table S2, Assignment of the protons of **SNAFR-1** via a 2D COSY.
Page S37	Table S3, Assignment of the protons of **SNAFR-2** via a 2D COSY.
	Table S4, Assignment of the protons of compound **12** via a 2D COSY.
Page S38	Table S5, Assignment of the protons of compound **19** via a 2D COSY.
	Table S6, Assignment of the protons of **SNAFR-1** H_2O adduct via a 2D COSY.

Introduction

During further investigations of the series of benzofluorones, we found that the original assignment of **SNAFR-1** as a mixture of tautomers based on ^{1}H NMR evidence was incorrect. The corrected assignment is a mixture of the regioisomers **SNAFR-1** and **SNAFR-2**, in a proportion of 1:2.5, respectively, based on NMR integral areas. The formation of **SNAFR-2** during the **SNAFR-1** synthesis is unexpected. Current investigations are ongoing. Both **SNAFR-1** and **SNAFR-2** were recently prepared by us via alternative synthetic routes (Scheme S1, page S5). Their corrected structure assignments were confirmed by extensive spectroscopic investigations including 2D COSY (Figure S1-

2, page S7). The **SNAFR-2** assignment was further confirmed by X-ray crystallography (Figure S3, page S8). The purity of all new compounds was studied via HPLC.

SNAFR-1 is more susceptible to nucleophilic attack by MeOH or H_2O as compared to **SNAFR-2**. When dissolved in MeOH-d_4, **SNAFR-1** converts to its MeOH-d_4 adduct (compound **19,** Scheme S2, page S8), the only species observed in the ^{1}H NMR spectrum (Figure S4, page S8). The conversion can be readily monitored via HPLC (Figure S21, page S22). **SNAFR-1** MeOH adduct (compound **18**) is obtained by dissolving **SNAFR-1** in MeOH followed by evaporation under vacuum.

In our previously published work, the stock solution of **SNAFR-1** and **SNAFR-2** regioisomers was prepared in MeOH. Therefore, the spectroscopic results originally reported in the text were the result of a mixture of **SNAFR-1** MeOH adduct and **SNAFR-2**. **SNAFR-1** MeOH adduct is shown to display a predominantly violet-blue emission in DMSO and MeOH (Figure S5, page S9). If MeOH is avoided during the sample preparation, the DMSO solution of **SNAFR-1** displays a violet-blue (from the H_2O adduct) as well as an orange (from the neutral form) and a near infra red (from the anionic form) emission (Figure S6, page S9). Due to the fact that the Hamamatsu R928 photomultiplier tube in our fluorimeter has a relatively low sensitivity in the NIR region, the intensity of NIR emission from **SNAFR-1** is significantly underestimated.

SNAFR-2 is not as susceptible to nucleophilic attack as **SNAFR-1**. **SNAFR-2** in MeOH displays predominantly green emission from the neutral form (Figure S7A, page S9). **SNAFR-2** in DMSO displays two-band emission from the H_2O adduct and neutral form of the compound (Figure S7B, page S9) although the adduct emission is relatively small. The reappearance of the adduct emission in DMSO is presumably due to the fact that DMSO, a polar aprotic solvent, facilitates nucleophilic attack from trace amounts of water present in DMSO. When 0.25% 50 mM phosphate buffer at pH 7.5 is added, both emissions from the adduct and anionic form are enhanced as a result of the increased amount of OH^- in the system leading to three band emissions of approximately equal intensities when excited in the UV region (red, green and violet-blue, Figure S8, page S10). **SNAFR-2** displays the same pH-responsive behavior when 0.25% 50 mM phosphate buffer is added to its DMSO solution as compared

to the published data in the original text (Figure S9, page S10). The same isosbestic points as originally reported were observed at 311, 345, 427, and 538 nm. It is interesting to note that the adduct emission from the **SNAFR-2** H_2O adduct is located at 360 nm instead of the originally reported 390 nm. It is apparent that the violet-blue emission originally reported in the text under the same conditions is largely from **18**. As a result of a 30 nm blue-shift of the violet-blue emission, the emission from **SNAFR-2** appears more yellow instead of near white (Figure S8, page S10). However, we have noted that the violet-blue emission at 390 nm from **SNAFR-2** is enhanced by activation of the central carbon via addition of dilute HCl followed by MeOH to generate the **SNAFR-2** MeOH adduct (Scheme S3, page S11). The **SNAFR-2** H_2O adduct may also be enhanced as well. The ratio of green and red emissions is further fine-tuned by addition of various amounts of phosphate buffer at different pH values, leading to the regeneration of near white emission from **SNAFR-2** (Figure S10, Page S11).

Additionally, the structural correction does not affect the spectroscopic measurements for applications such as ratiometric pH studies (Figure S11, Page S11) or live cell imaging. Identical green and red peak locations at 540 and 620 nm in 50 mM phosphate buffer are observed as in the published text, which result from the neutral and anionic forms of **SNAFR-2,** respectively (rather than from **SNAFR-1** as originally reported). Moreover, the pK_a of **SNAFR-2** is essentially the same as the published data (previously assigned to **SNAFR-1**) based on absorption and fluorescence titration data.

Experimental Section

Scheme S1. Alternative syntheses of **SNAFR-1** and **SNAFR-2** affording pure regioisomers for structural studies and spectroscopic investigations.

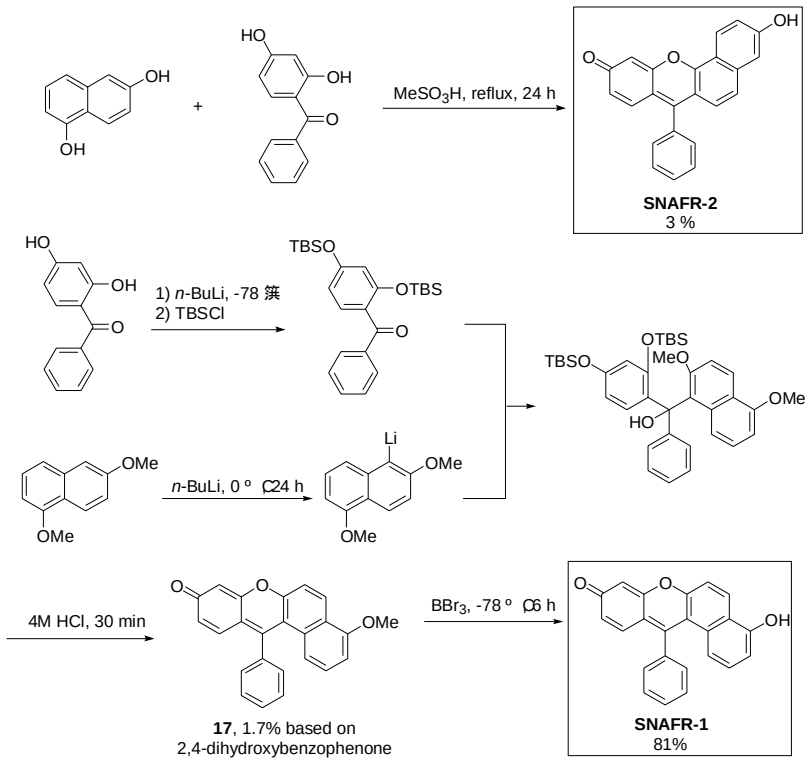

Alternative Synthesis of SNAFR-1. 2,4-Dihydroxybenzophenone (2.0 g, 9.3 mmol) is dissolved in THF (100 mL). The solution is cooled to -78 ºC with a dry ice bath. *n*-BuLi (11.6 mL, 1.6 M in hexane) is added dropwise with constant stirring. The mixture is allowed to warm to rt overnight and cooled over an ice bath**.** TBDMSCl (2.9 g, 19.5 mmol) in THF (20 mL) is added dropwise. After the addition is complete, the solution is allowed to warm to rt within 4 h. The solution is re-cooled to -78 ºC and a solution of lithiated 1,6-dimethoxynaphthalene (1.84 g, 9.8 mmol, see original supporting information for preparation of the solution) is added dropwise. After completion, the solution is allowed to warm to rt overnight. HCl (10 mL, 4 M) is added in one portion. The solution is stirred at rt for 30 min. Deionized H_2O (200 mL) is added. Much of the THF is removed under vacuum. The remaining aqueous material is extracted with CH_2Cl_2 and dried over $MgSO_4$. Purification by flash chromatography (EtOAc) affords 56 mg (1.7 % yield based on 2,4-dihydroxybenzophenone, yield not yet optimized) of new **SNAFR-1** methyl ether (**17**). 18 mg of **17** is dissolved in anhydrous CH_2Cl_2. The

solution is cooled over a dry ice bath. The remaining methyl group is removed via addition of 0.3 mL BBr_3 to obtain 14 mg (81% yield) of **SNAFR-1**.

Data for compound **17**: ^{1}H NMR (DMSO-d_6, 300 MHz) δ (ppm): 8.58 (d, J = 9.2 Hz, 1H), 7.72 (d, J = 9.2 Hz, 1H), 7.66–7.69 (m, 3H), 7.44-7.48 (m, 2H), 7.11 (d, J = 8.4 Hz, 1H), 7.01 (d, J = 10.0 Hz, 1H), 6.97 (d, J = 7.8 Hz, 1H), 6.65 (d, J = 8.8 Hz, 1H), 6.51 (dd, J = 10.0, 2.0 Hz, 1H), 6.31 (d, J = 2.0 Hz, 1H), 3.95 (s, 3H). ^{13}C NMR (DMSO-d_6, 75 MHz) δ (ppm): 183.1, 157.1, 155.3, 153.2, 148.8, 136.3, 130.1, 129.7, 129.3, 129.0, 128.2, 127.8, 127.5, 125.0, 117.2, 116.0, 104.8, 103.4, 55.7. MALDI-TOF $[M+H]^+$ calcd 353.117, found 353.330.

Data for **SNAFR-1**: ^{1}H NMR (DMSO-d_6, 300 MHz) δ (ppm): 8.58 (d, J = 9.3 Hz, 1H), 7.68-7.69 (m, 3H), 7.66 (d, J = 9.3 Hz, 1H), 7.44-7.48 (m, 2H), 7.00 (d, J = 9.9 Hz, 1H), 6.98 (dd, J = 8.4, 7.2 Hz, 1H), 6.84 (d, J = 7.2 Hz, 1H), 6.51 (dd, J = 9.9, 1.8 Hz, 1H), 6.43 (d, J = 9.3 Hz, 1H), 6.32 (d, J = 1.8 Hz, 1H). ^{13}C NMR (DMSO-d_6, 75 MHz) δ (ppm): 183.1, 157.2, 154.0, 149.2, 136.4, 130.8, 130.2, 130.1, 129.7, 128.9, 129.0, 128.1, 120.0, 115.9, 115.2, 108.5, 103.3. MALDI-TOF $[M+H]^+$ calcd 339.102, found 339.319.

Synthesis of SNAFR-2. 1,6-Dihydroxynaphthalene (1.5 g, 9.3 mmol) and 2,4-dihydroxybenzophenone (2.0 g, 9.3 mmol) are added to a 100 mL round bottom flask containing 25 mL CH_3SO_3H. The mixture is heated at reflux for 24 h. The resulting dark-red liquid is poured into 200 mL distilled H_2O and neutralized by the addition of $NaHCO_3$ until the solution turns almost colorless. The liquid is decanted and the resulting residue is dissolved in MeOH and treated with Na_2SO_4. The mixture is filtered and evaporated to dryness. The red residue is purified by flash chromatography (EtOAc:MeOH=9.5:0.5). 18.6 mg (3 % yield, not optimized) **SNAFR-2** are obtained.

Data for **SNAFR-2**: ^{1}H NMR (DMSO-d_6, 300 MHz) δ (ppm): 8.52 (d, J = 9.3 Hz, 1H), 7.65-7.70 (d, 3H), 7.56 (d, J = 9.0, 1H), 7.49-7.53 (m, 2H), 7.32 (dd, J = 9.3, 2.7 Hz, 1H), 7.23 (d, J = 2.7 Hz, 1H), 7.09 (d, J = 9.3 Hz, 1H), 7.04 (d, J = 9.0, 1H), 6.52 (dd, J = 9.3, 1.5 Hz, 1H), 6.50 (d, J = 1.5 Hz, 1H). ^{13}C NMR (DMSO-d_6, 75 MHz) δ (ppm): 183.5, 159.6, 158.3, 150.0, 137.7, 132.7, 130.3, 130.0, 129.4,

128.8, 124.6, 123.5, 123.2, 119.9, 116.0, 113.5, 110.0, 104.7. MALDI-TOF $[M+H]^+$ calcd 339.102, found 339.431.

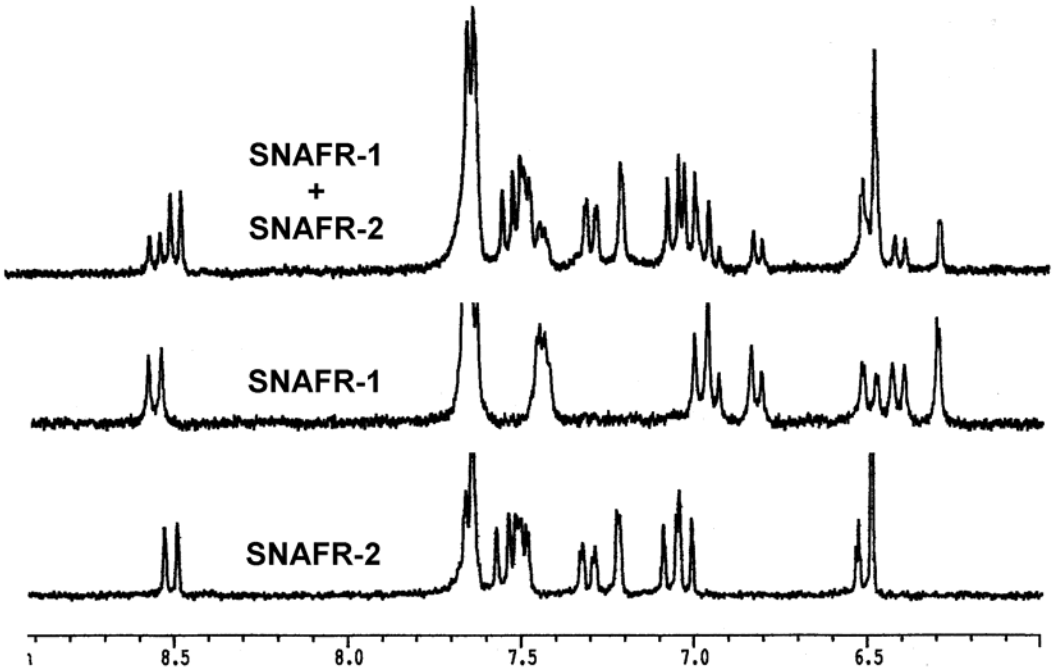

Figure S1. Top: ^{1}H NMR spectrum of the mixture of **SNAFR-1** and **SNAFR-2** which was believed to contain a tautomeric mixture of **SNAFR-1**. Center: Pure **SNAFR-1** derived from the alternative synthetic route described above. Bottom: Pure **SNAFR-2** from the synthetic route described above. Further characterization data and evidence of purity is shown on the following pages.

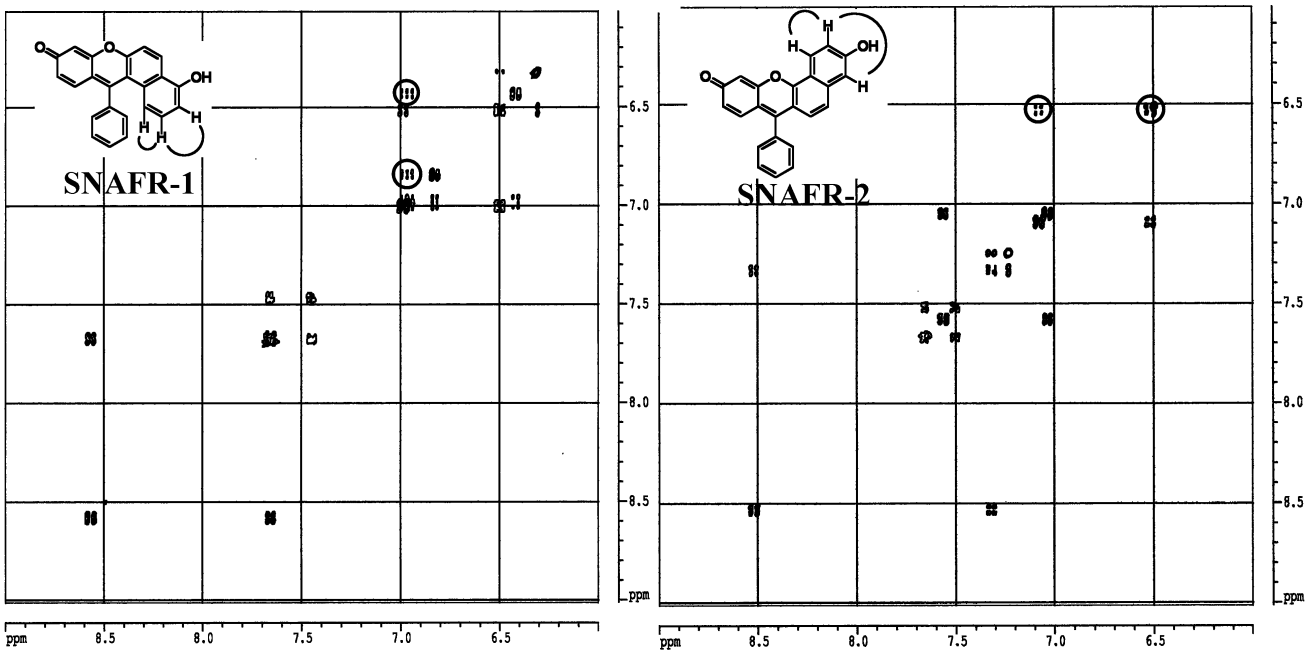

Figure S2. 2D COSY of **SNAFR-1** (left) and **SNAFR-2** (right) in DMSO-d_6 (expansion from 6.0 to 9.0 ppm). Characteristic cross-crouplings are circled for clarity. Please find detailed assignment including chemical shift, coupling constant and splitting pattern in Table S2 and Table S3. The scales are shown without the proton NMRs which correspond to those shown in Figure S1, above.

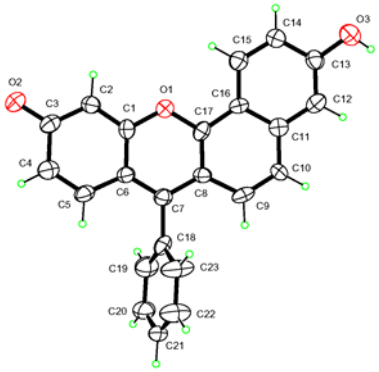

Figure S3. Ortep drawing of the single crystal X-ray structure of **SNAFR-2**.

Scheme S2. Quantitative conversion of **SNAFR-1** to its MeOH or MeOH-d_4 adducts.

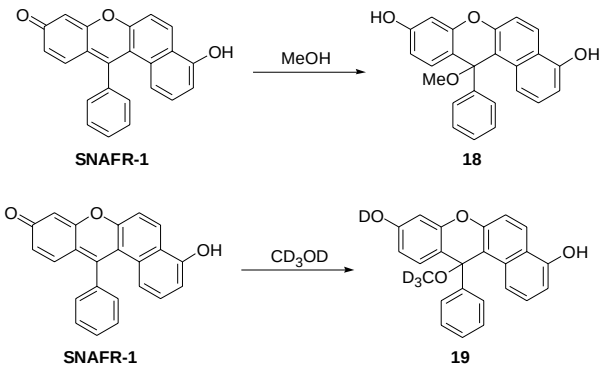

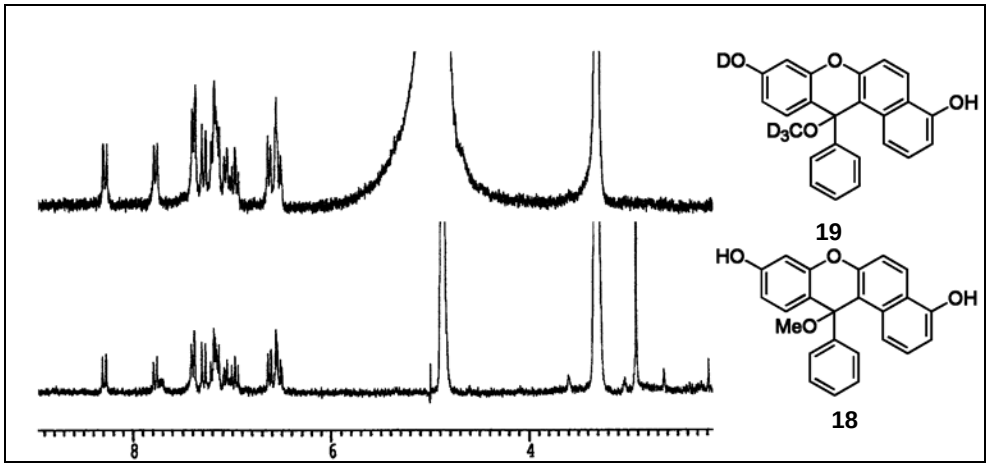

Figure S4. Overlay of the ^{1}H NMR spectra in MeOH-d_4 of new compounds **18** and **19**. The methyl peak at 2.92 ppm observed in the NMR of compound **18** is not found in the NMR of compound **19** as expected. See also HPLC data (Figure S20, Page S22) which allows one to follow the facile conversion of **SNAFR-1** to its MeOH adduct.

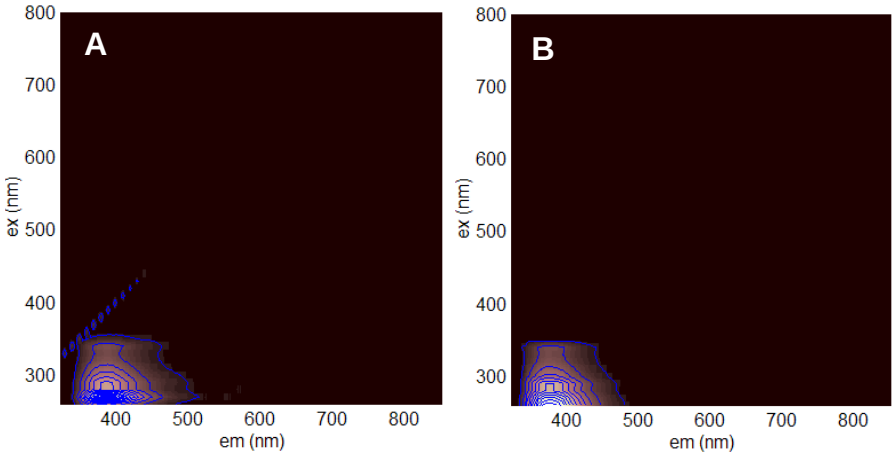

Figure S5. Excitation emission matrices (EEMs) of **18** in various solvents. (A) in MeOH and (B) in DMSO. Solutions of **SNAFR-1** were prepared from a MeOH stock solution and dried before reconstitution in the desired solvent. Data are normalized to the maximum emission in each EEM respectively. Only significant violet-blue emission is observed in each solvent.

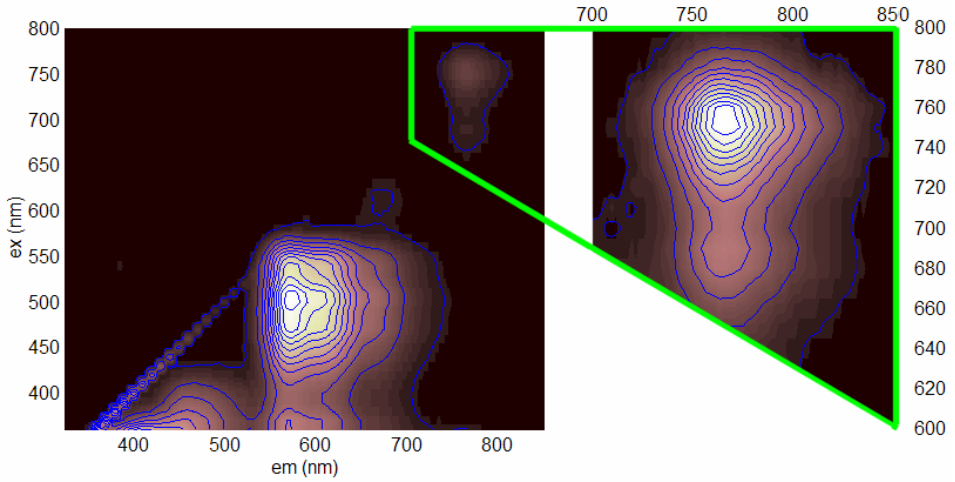

Figure S6. EEM of **SNAFR-1** in DMSO prepared from a DMSO stock solution. Blue, orange and NIR emissions are observed when excited at various wavelengths. MeOH was avoided in stock solution preparation to minimize adduct formation. The intensity of the NIR band shown above is underestimated due to the relatively low sensitivity of the photomultiplier tube used in this study.

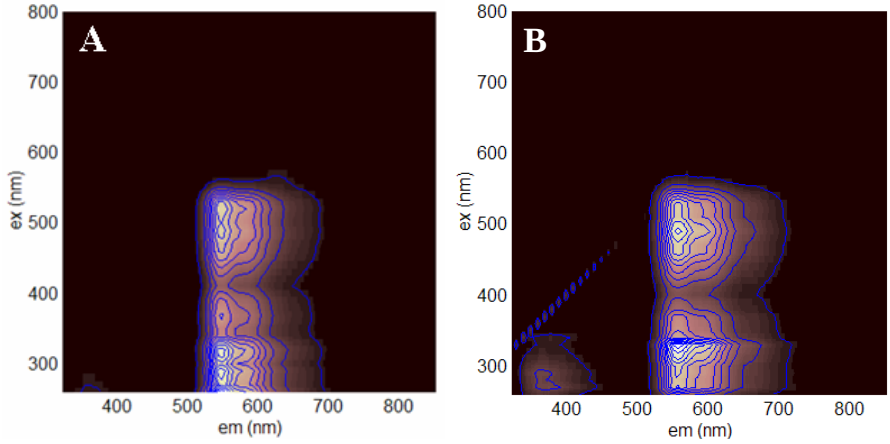

Figure S7: EEMs of the **SNAFR-2** and its adducts in various solvents. (A) in MeOH, (B) in DMSO,. Solutions of **SNAFR-2** were prepared from a MeOH stock solution and dried before reconstitution in

the desired solvent. Data are normalized to the maximum emission in each EEM respectively. Green emission is observed in MeOH solution. Violet-blue and green emissions are observed in DMSO solution.

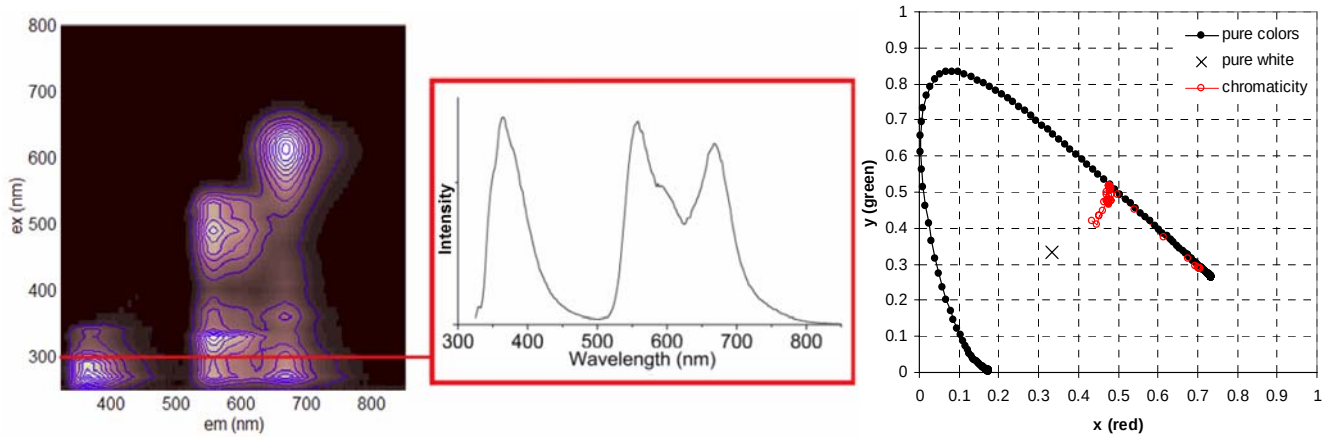

Figure S8. Left: EEM of the **SNAFR-2** in DMSO with 0.25% 50 mM phosphate buffer at pH 7.5. Middle: Emission spectrum of **SNAFR-2** (30 μM, 0.25 % 50 mM phosphate buffer, pH 7.5, in DMSO) when excited at 300 nm, displays violet-blue, green and red emissions of approximately equal intensities. Right: Chromaticity coordinates for emission spectra collected with excitation wavelength between 270 nm and 650 nm for the corresponding solution.

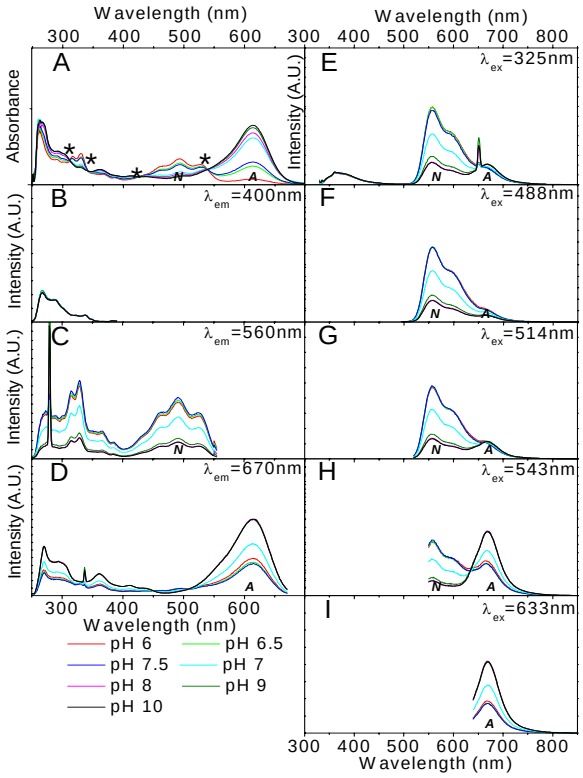

Figure S9: Titration of **SNAFR-2** in 99.75% DMSO with 0.25% 50 mM phosphate buffer at various pH. ***A*** = Anionic form. ***N*** = Neutral form. (A) Absorption spectra. The * in Figure A indicates the positions of isosbestic points in absorbance spectra. (B-D) Excitation spectra with emission monitored at 400 nm, 560 nm and 670 nm respectively. (E-I) Emission spectra excited at 325 nm, 488 nm, 514 nm, 543 nm and 633 nm respectively corresponding to common laser lines. The pH-responsive ratiometric green and red emissions are the result of **SNAFR-2.**

Scheme S3: Protonation of **SNAFR-2** by dilute acid facilitates the nucleophilic addition of MeOH.

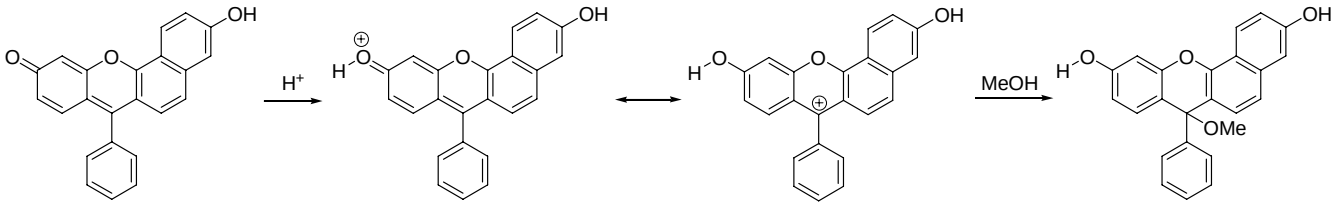

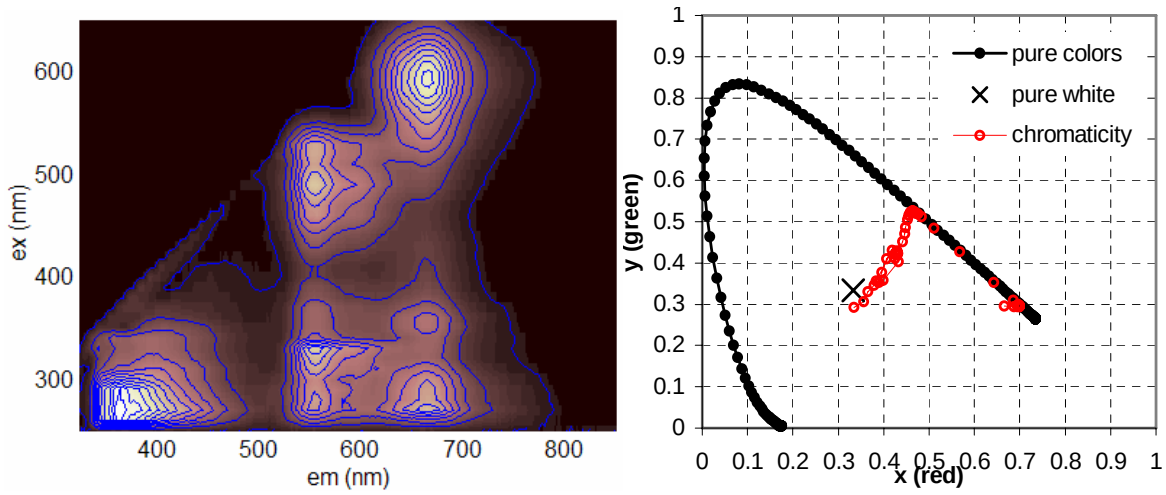

Figure S10: Left: EEM of a solution of **SNAFR-2** (1 ml, 30 µM in DMSO) after addition of HCl (7 µl, 0.1 M), MeOH (0.05 mL) and then pH 7.5 phosphate buffer (60 µL, 50 mM). Right: Chromaticity coordinates for emission spectra collected with excitation wavelength between 270 nm and 650 nm for the corresponding solution.

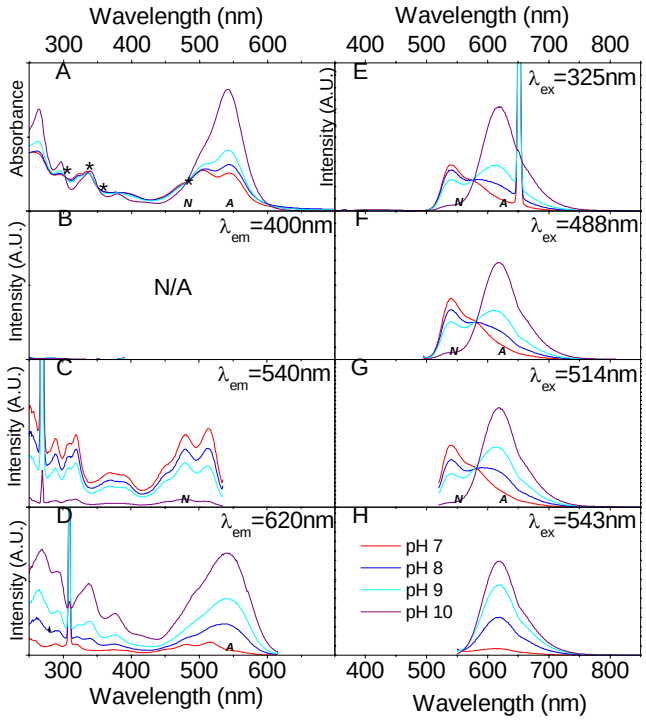

Figure S11: Titration of **SNAFR-2** in 99.75% 50 mM phosphate buffer with 0.25% DMSO. ***A*** = anionic form. ***N*** = neutral form. (A) Absorption spectra. The * indicates the position of isosbestic points.

(B-D) Excitation spectra with emission monitored at 400 nm, 540 nm and 620 nm respectively. (E-H) Emission spectra excited at 325 nm, 488 nm, 514 nm, and 543 nm respectively, corresponding to common laser lines. Legends for Figures A-H are shown in Figure H.

Figure S12: ^{1}H NMR of compound **17** in DMSO-d_6.

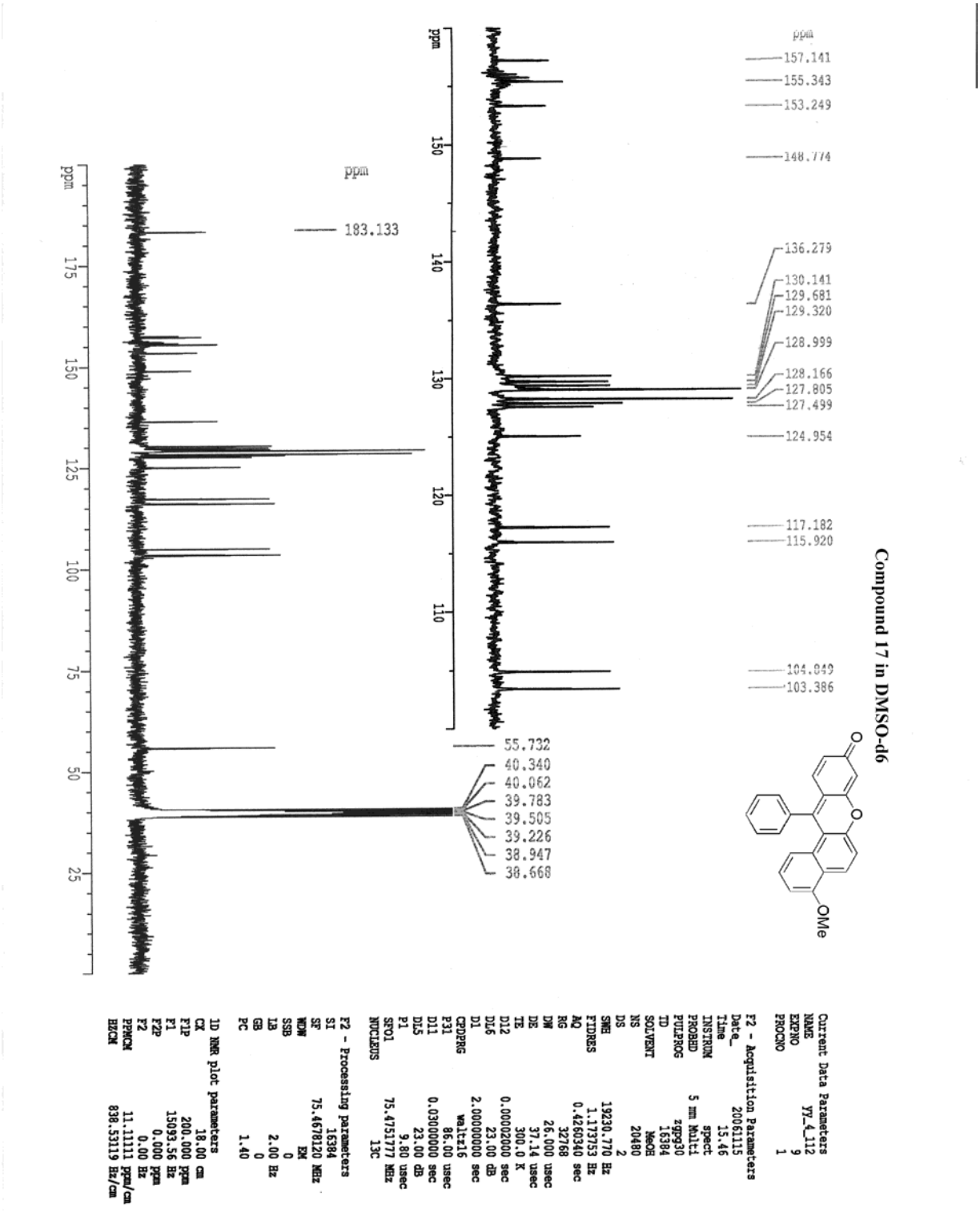

Figure S13: ^{13}C NMR of compound **17** in DMSO-d_6.

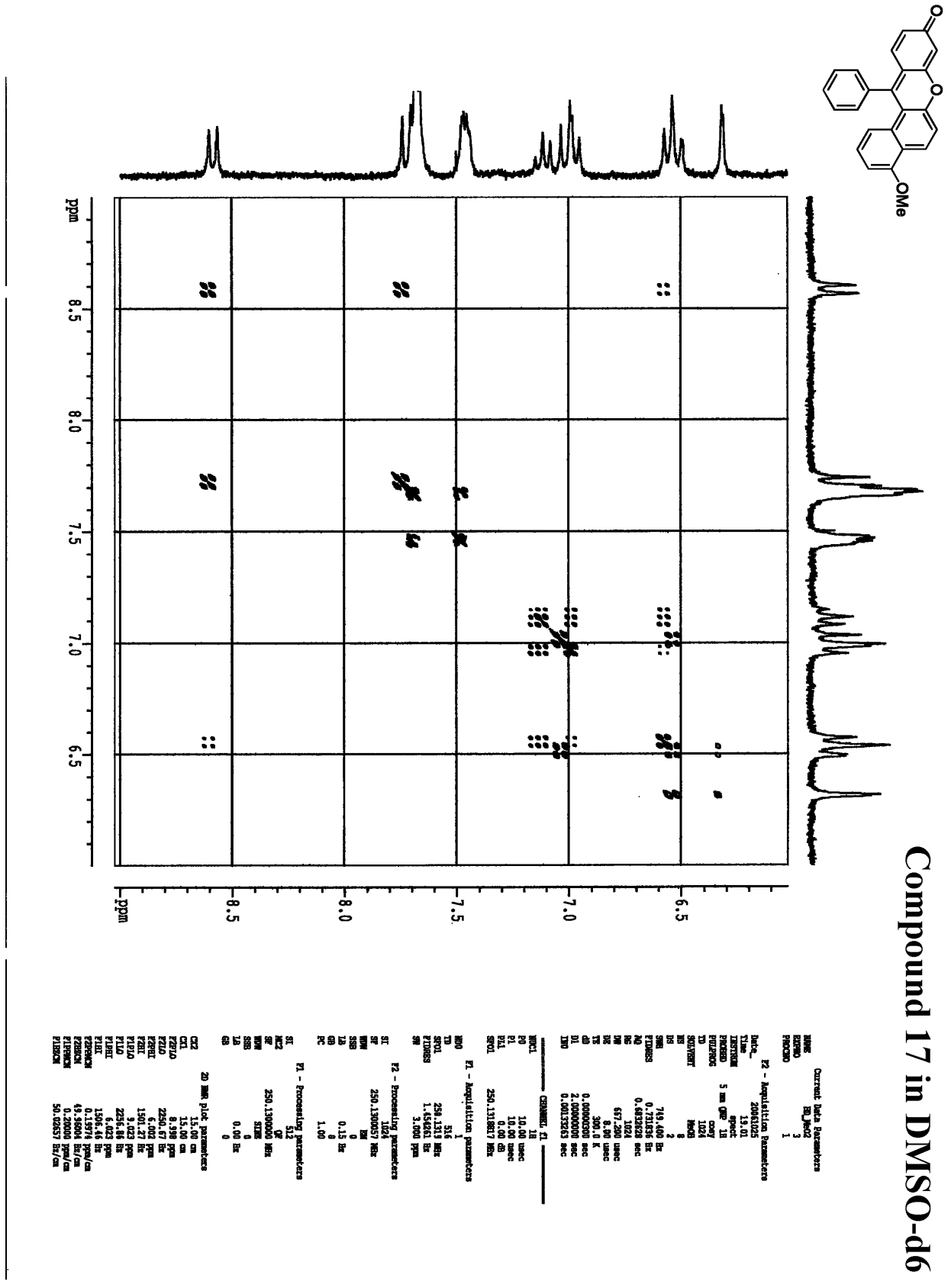

Figure S14: 2D-COSY of compound **17** (expansion from 6.0-9.0 ppm) in DMSO-d_6.

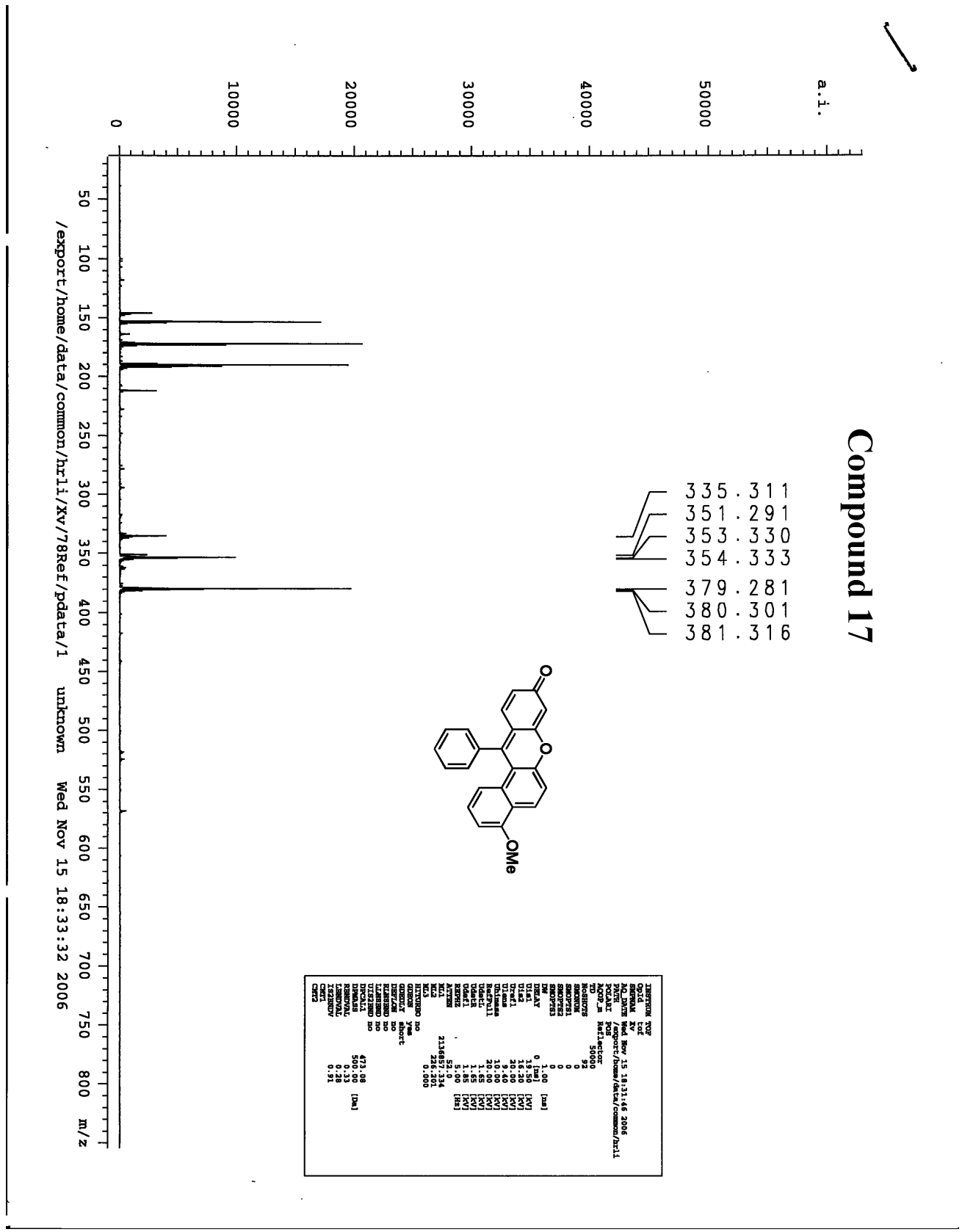

Figure S15: MALDI-TOF of compound **17**.

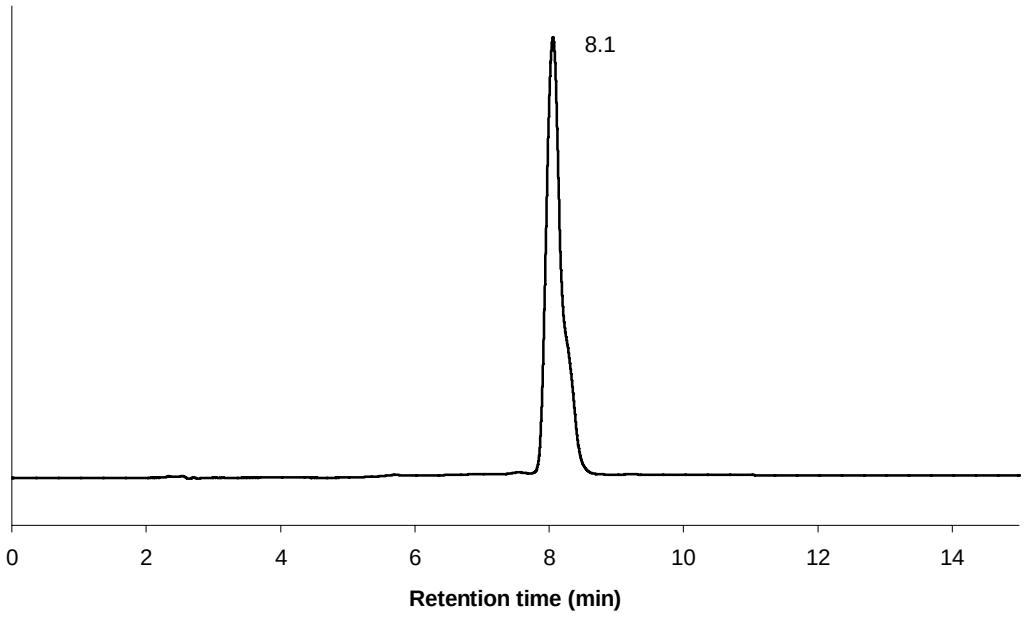

Figure S16: Chromatogram of a solution of **compound 17** in MeOH. HPLC purity screening is performed on a CM4000 multiple solvent delivery system connected to a SpectroMonitor 3100 UV-Vis detector (LDC/Milton Roy) using a LiChrospher 100 RP-18 (5 μm) endcapped column (250 × 4.6 mm). The flow rate is 1.0 mL/min and the detector wavelength is set to 490 nm. Mobile phase (gradient): 70/30 MeOH/H_2O to 100/0 % MeOH/H_2O in 5 min.

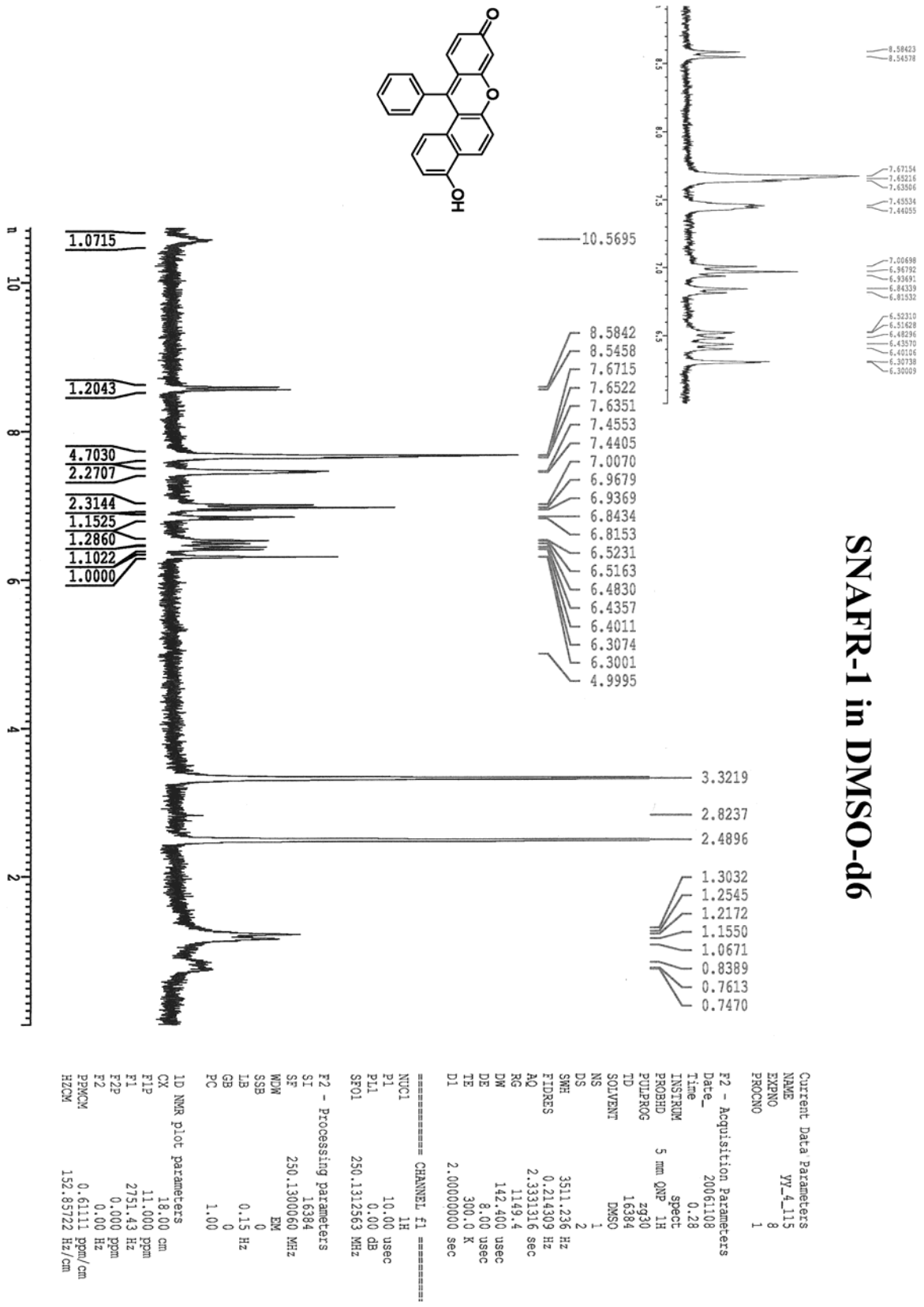

Figure S17: ^{1}H NMR of **SNAFR-1** in DMSO-d_6.

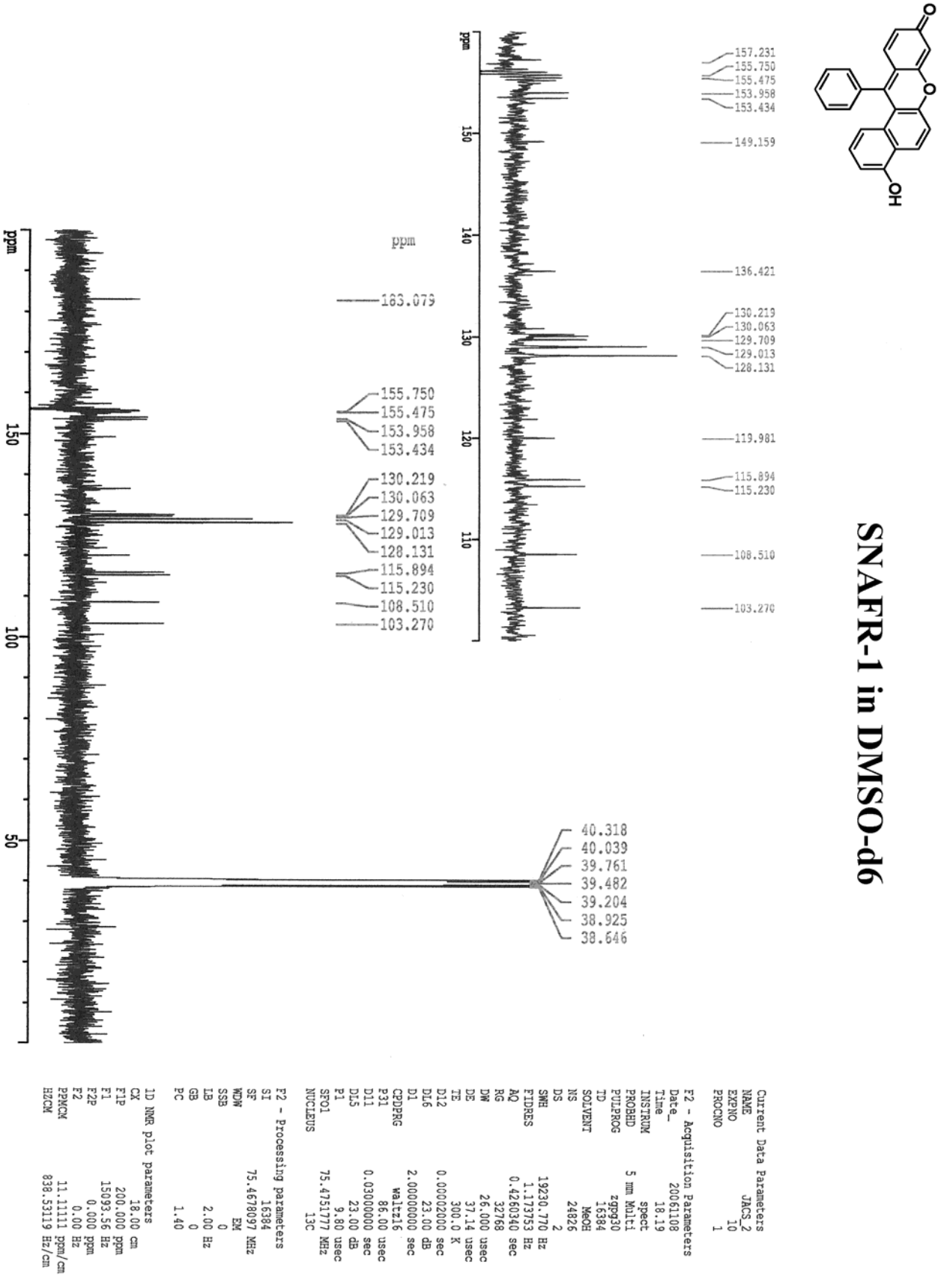

Figure S18: ^{13}C NMR of **SNAFR-1** in DMSO-d_6.

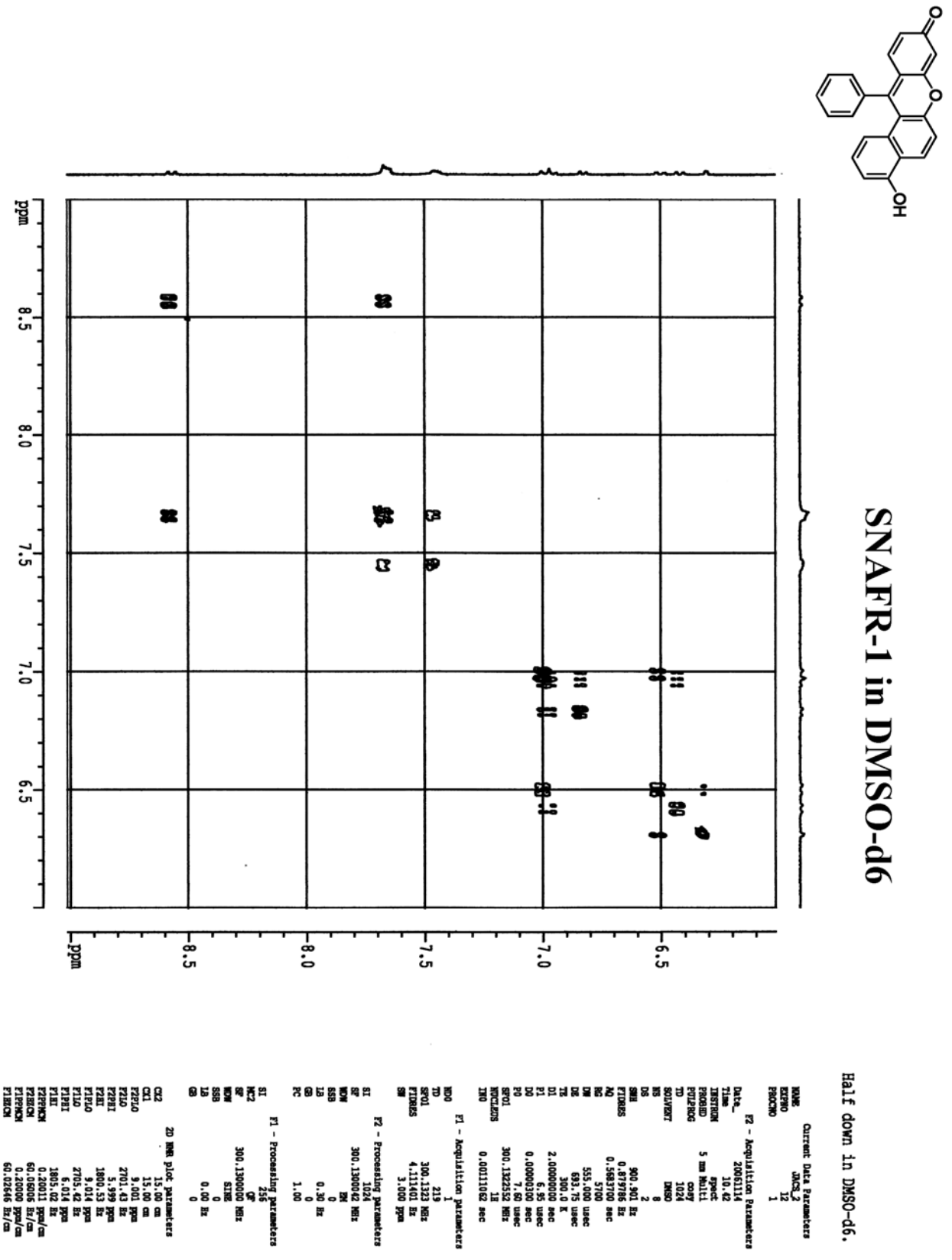

Figure S19: 2D-COSY of **SNAFR-1** (expansion from 6.0-9.0 ppm) in DMSO-d_6.

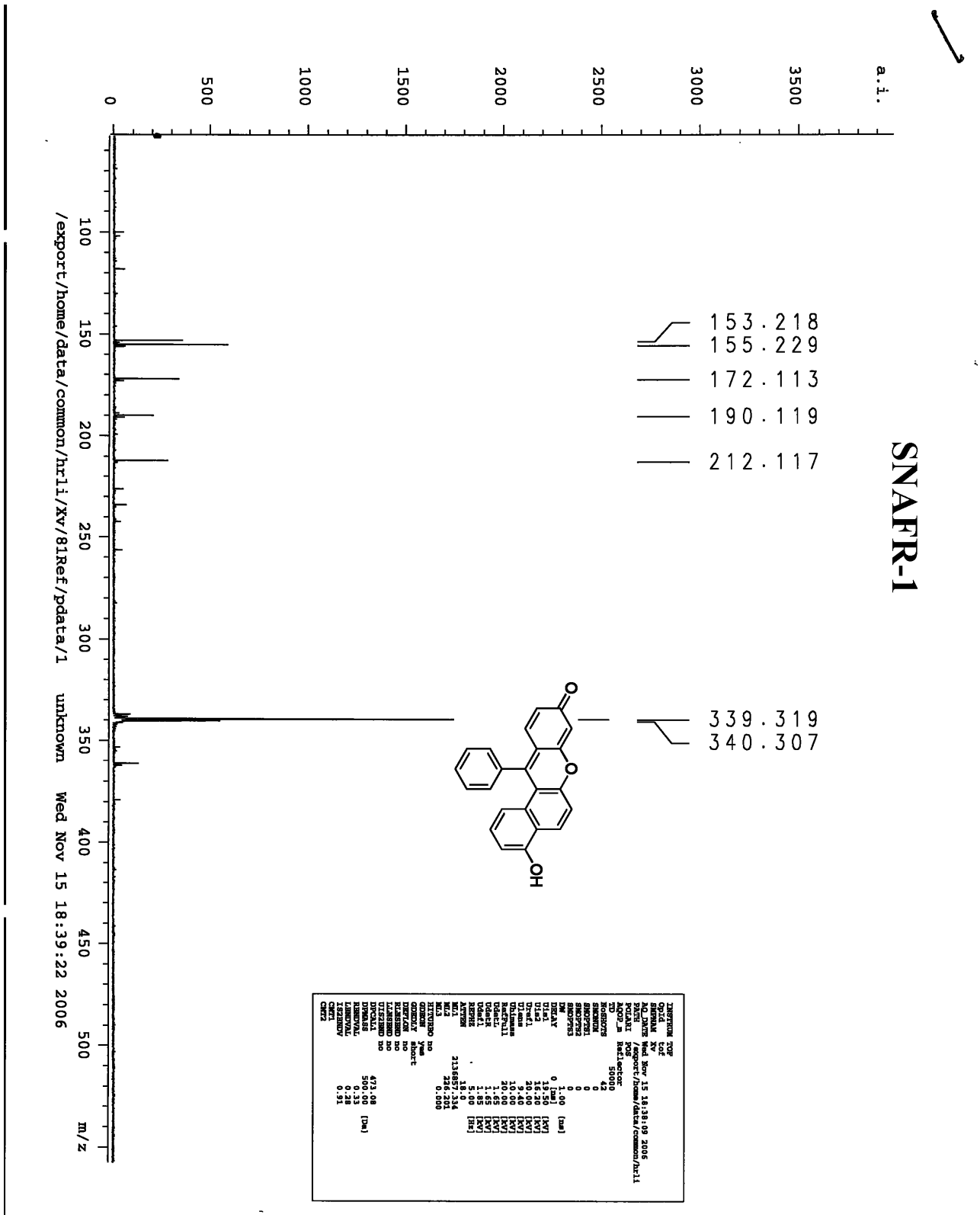

Figure S20: MALDI-TOF of **SNAFR-1**.

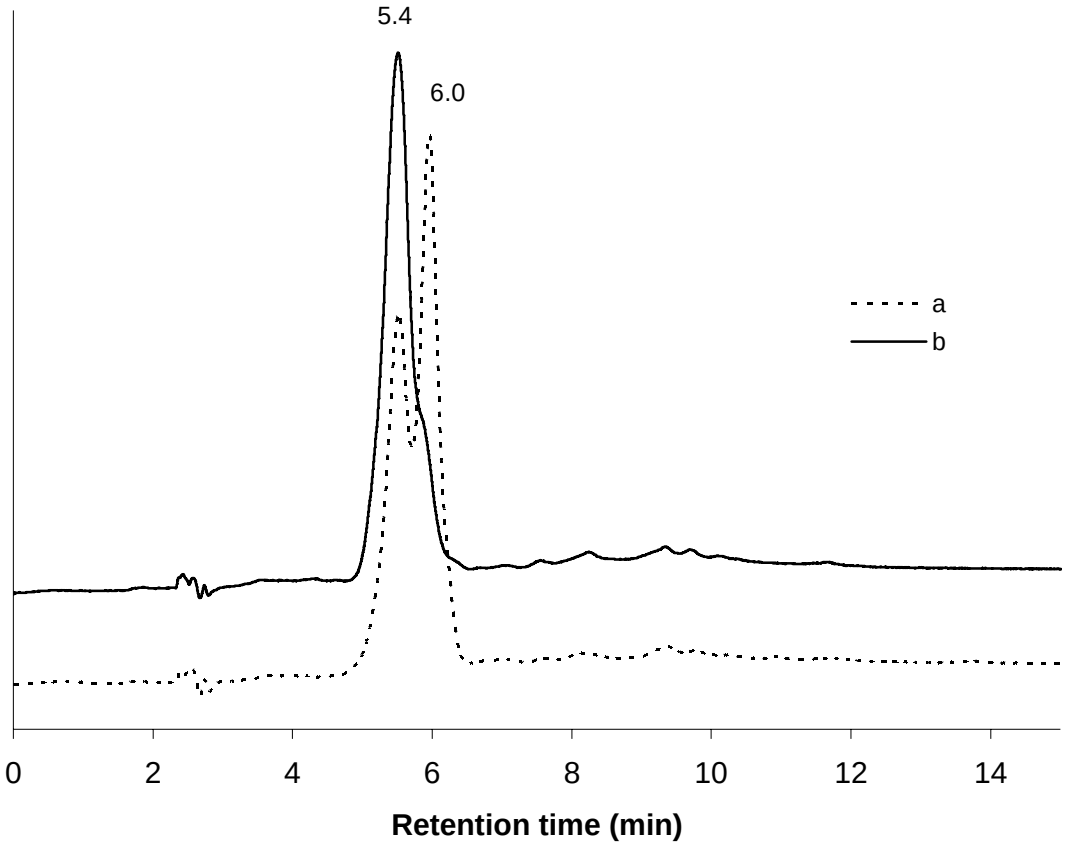

Figure S21. a) HPLC trace of freshly dissolved **SNAFR-1** in MeOH showing two peaks (retention times = 5.4 and 6.0 min, **SNAFR-1 MeOH adduct** and **SNAFR-1,** respectively). b) HPLC trace of **SNAFR-1**. **SNAFR-1** dissolved in MeOH after sitting in the dark for 30 min. Only the peak corresponding to the **SNAFR-1** MeOH adduct is observed showing that the MeOH present promotes the conversion of **SNAFR-1** to its MeOH adduct. HPLC analysis is performed on a CM4000 multiple solvent delivery system connected to a SpectroMonitor 3100 UV-Vis detector (LDC/Milton Roy) using a LiChrospher 100 RP-18 (5 μm) endcapped column (250 × 4.6 mm). The flow rate is 1.0 mL/min and the detector wavelength is set to 490 nm. Mobile phase (gradient): 70/30 MeOH/H_2O to 100/0 % MeOH/H_2O in 5 min.

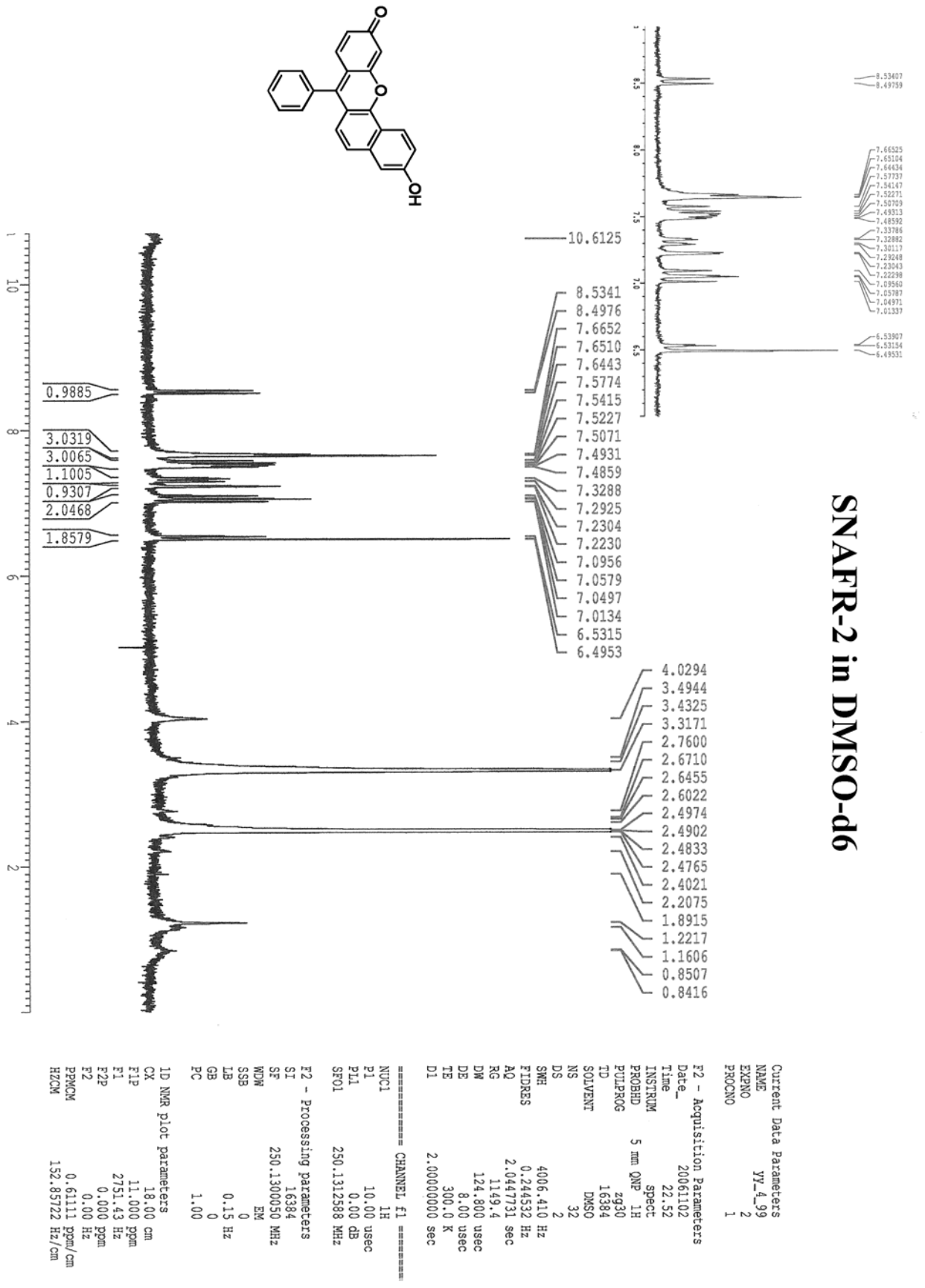

Figure S22: ^{1}H NMR of **SNAFR-2** in DMSO-d_6.

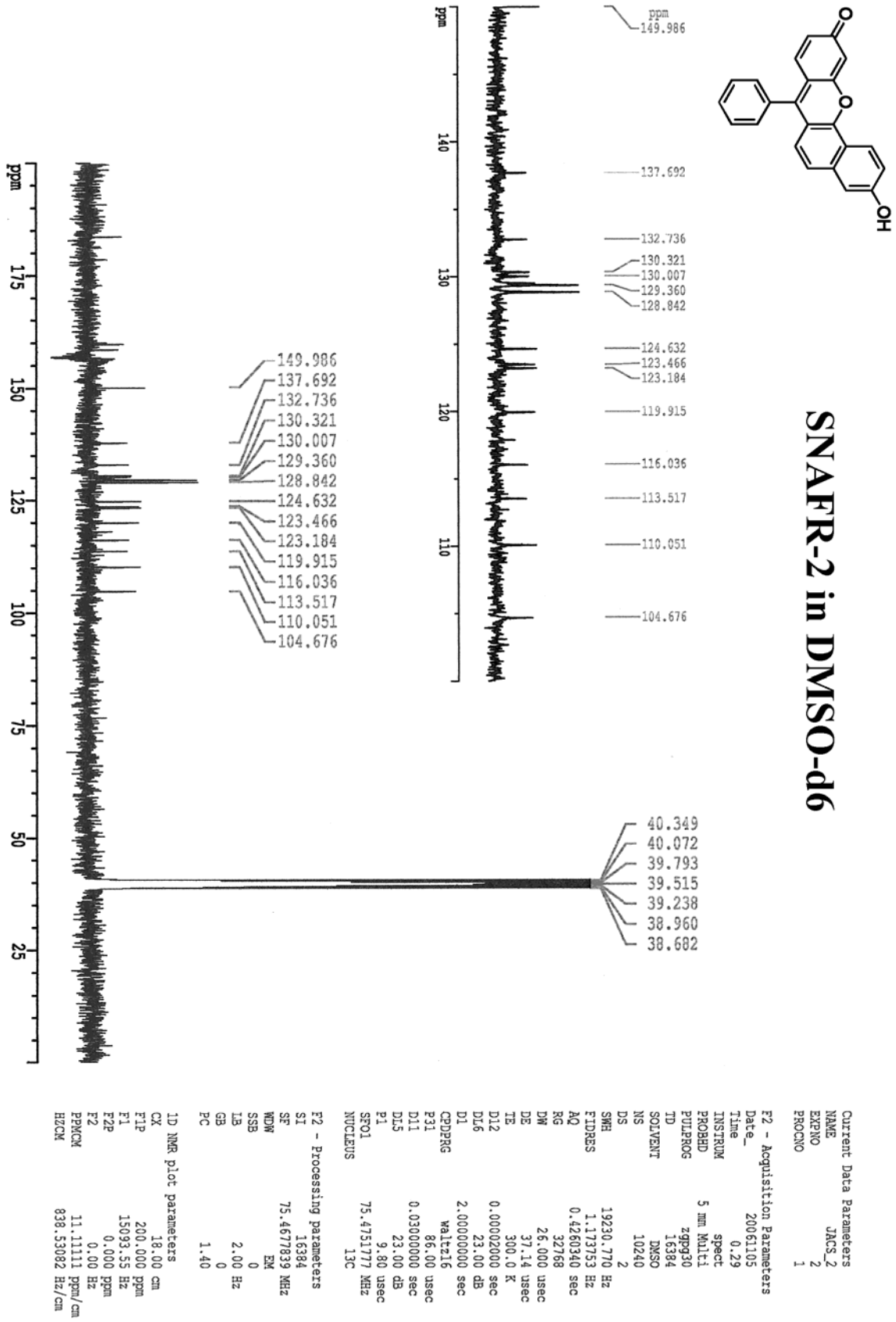

Figure S23: ^{13}C NMR of **SNAFR-2** in DMSO-d_6.

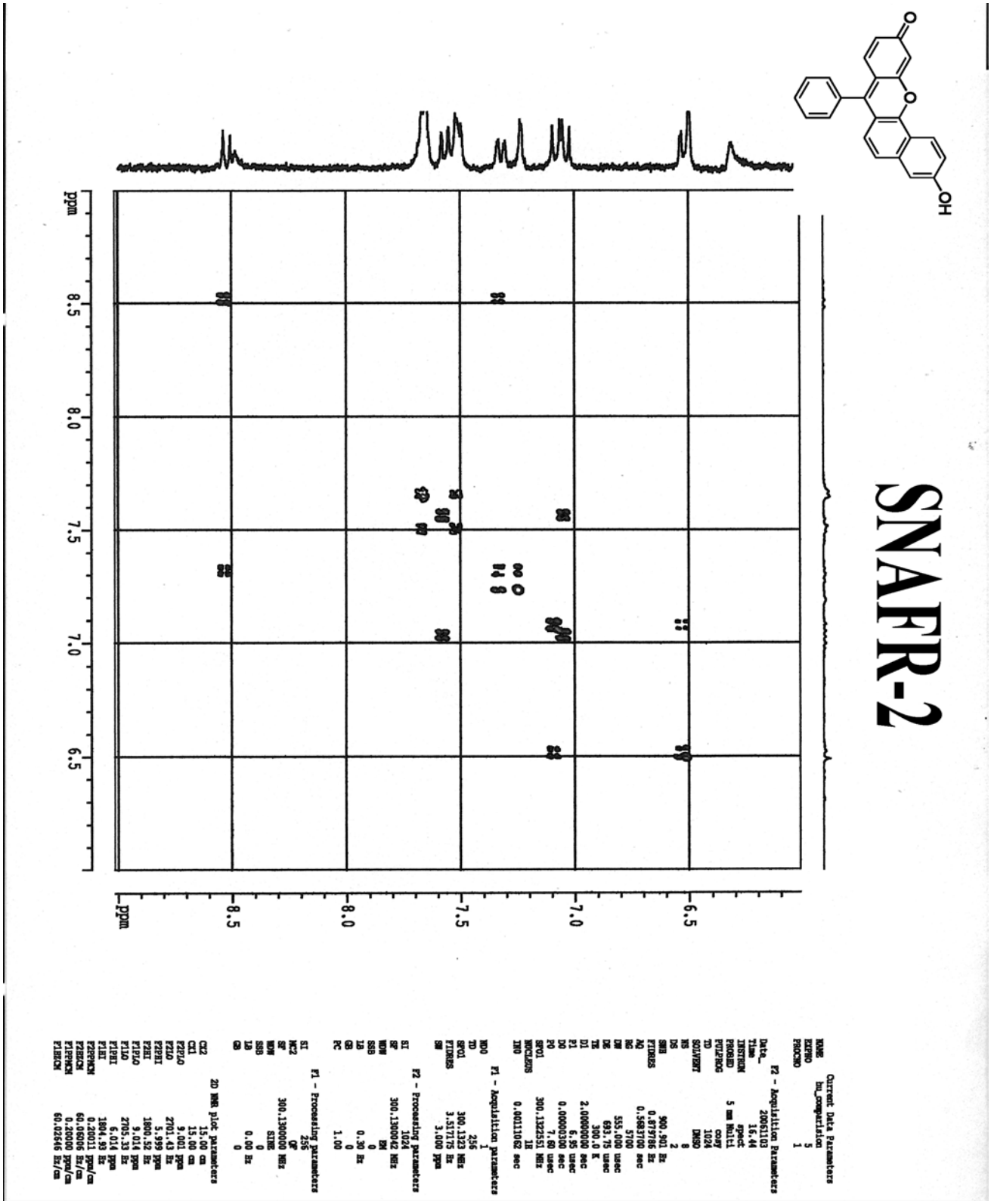

Figure S24: 2D-COSY of **SNAFR-2** (expansion from 6.0-9.0 ppm) in DMSO-d_6

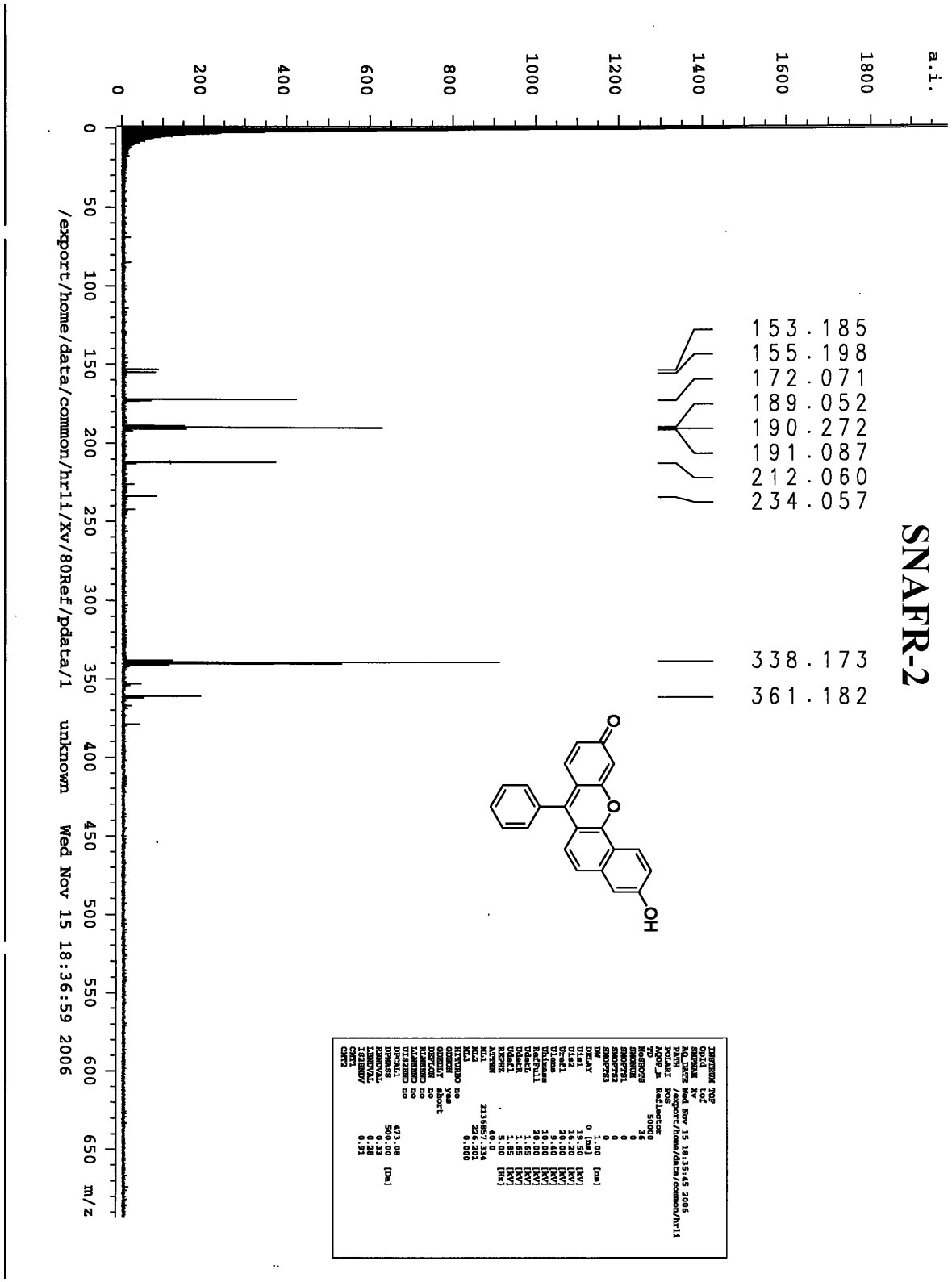

Figure S25: MALDI-TOF of **SNAFR-2**.

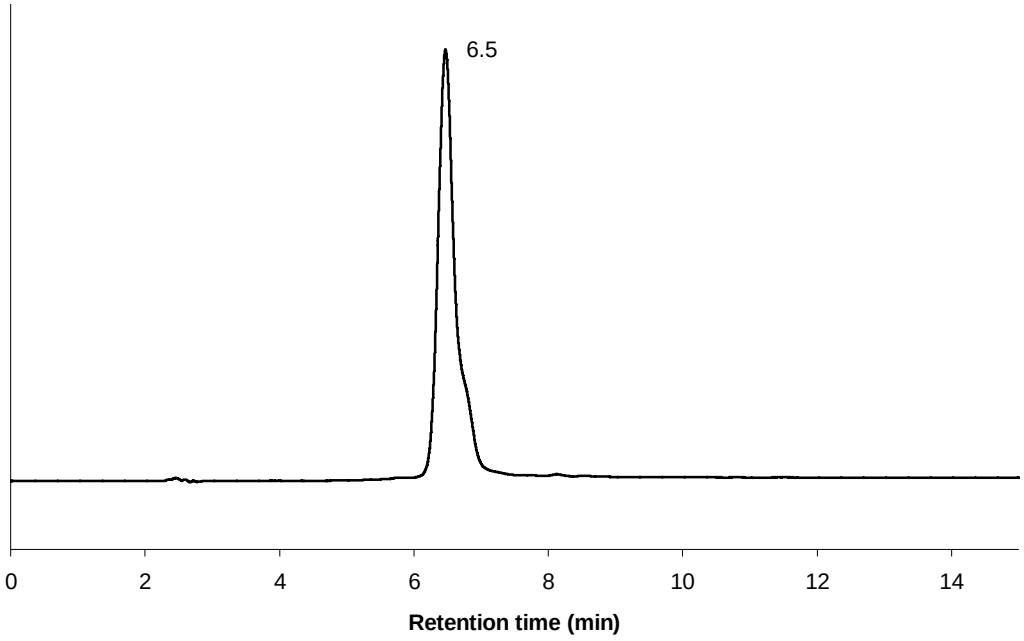

Figure S26: Chromatogram of a solution of **SNAFR-2** in MeOH. HPLC purity screening is performed on a CM4000 multiple solvent delivery system connected to a SpectroMonitor 3100 UV-Vis detector (LDC/Milton Roy) using a LiChrospher 100 RP-18 (5 μm) endcapped column (250 × 4.6 mm). The flow rate is 1.0 mL/min and the detector wavelength is set to 490 nm. Mobile phase (gradient): 70/30 MeOH/H_2O to 100/0 % MeOH/H_2O in 5 min.

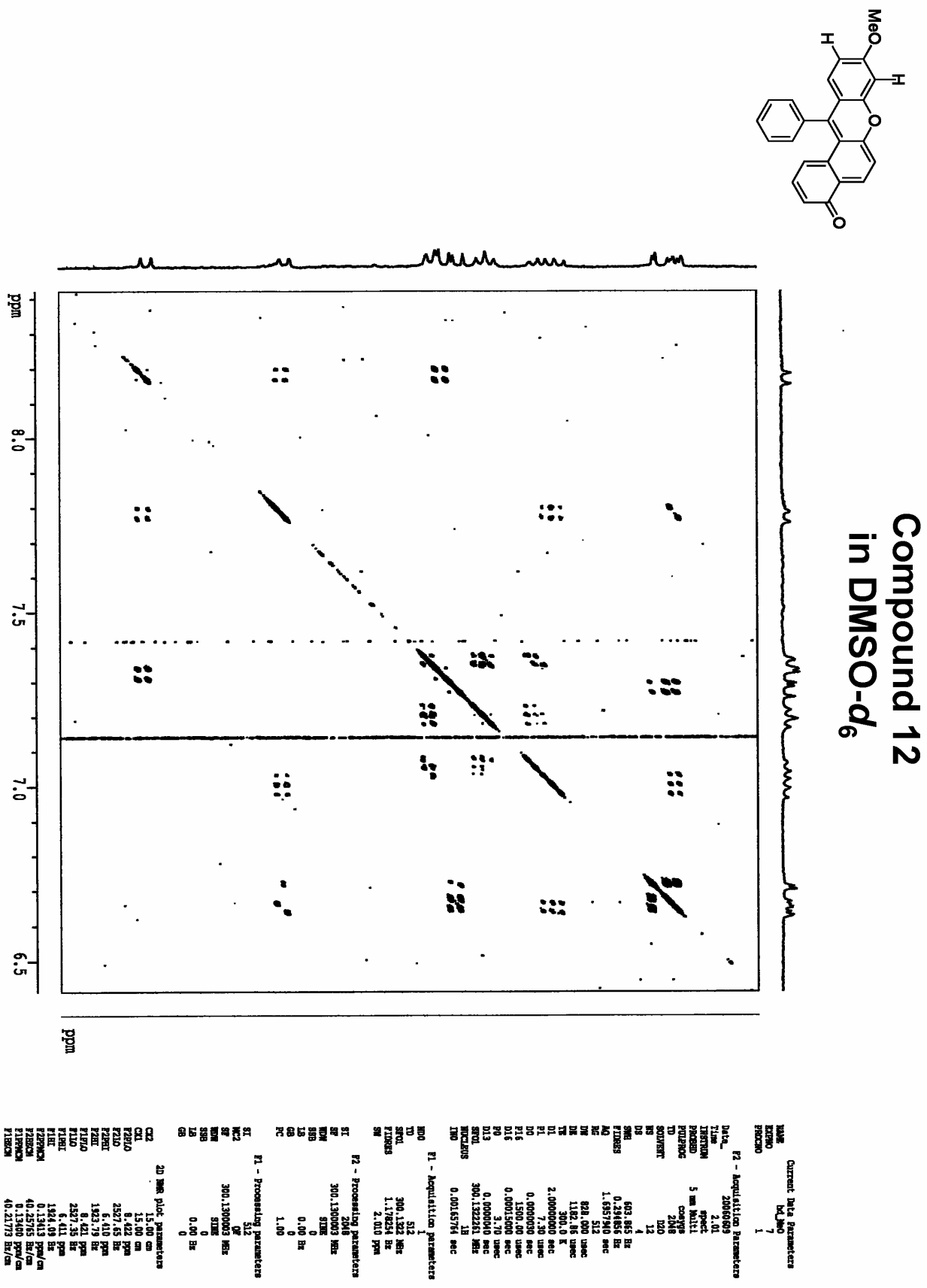

Figure S27: 2D-COSY of **compound 12** (expansion from 6.0-9.0 ppm) in DMSO-d_6

Compound 12

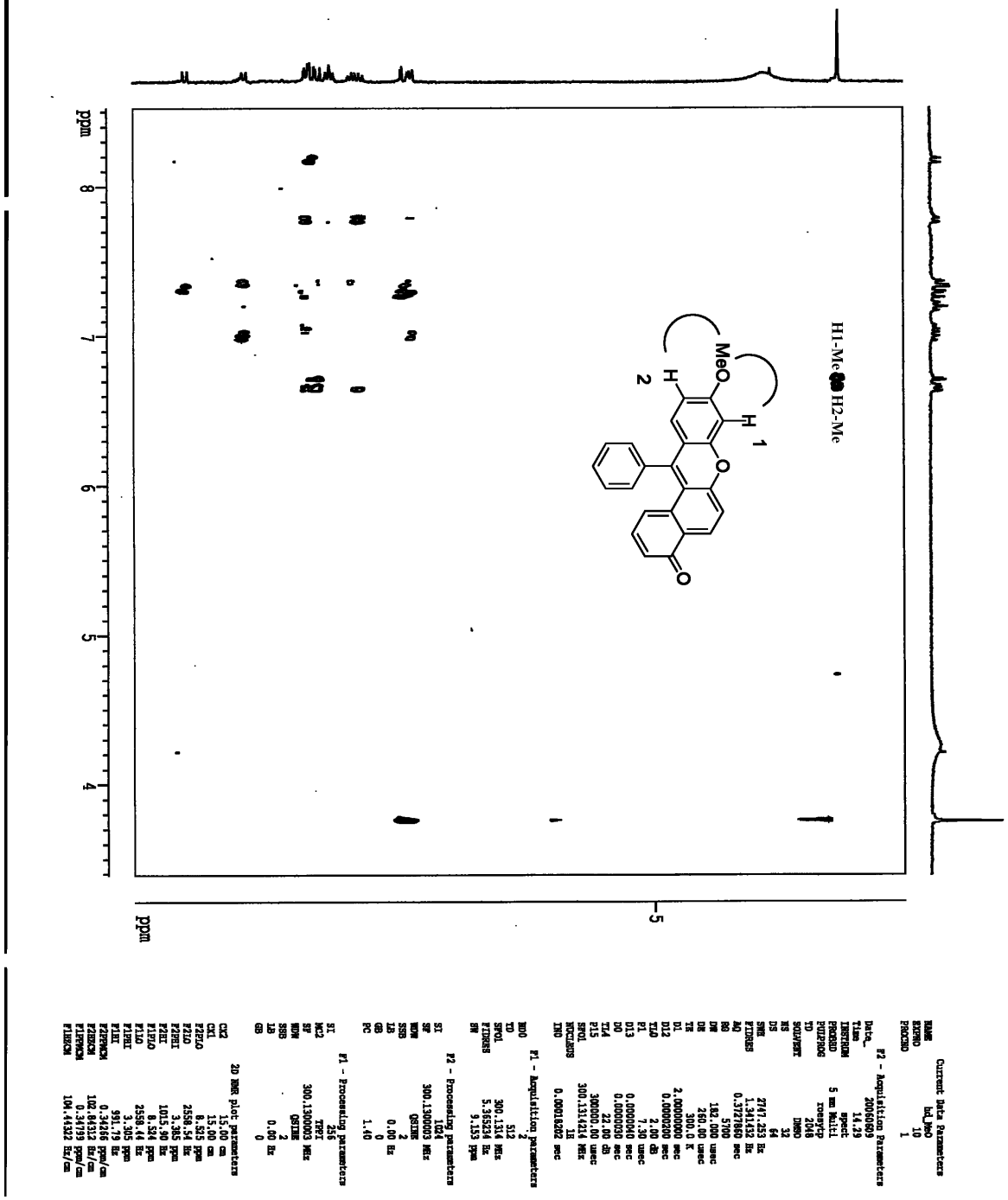

Figure S28: 2D-ROESY of **compound 12** (expansion from 6.0-9.0 ppm) in DMSO-d_6. The through-space coupling of H-1 and H-2 with Methyl group confirms the correct assignment of compound **12**.

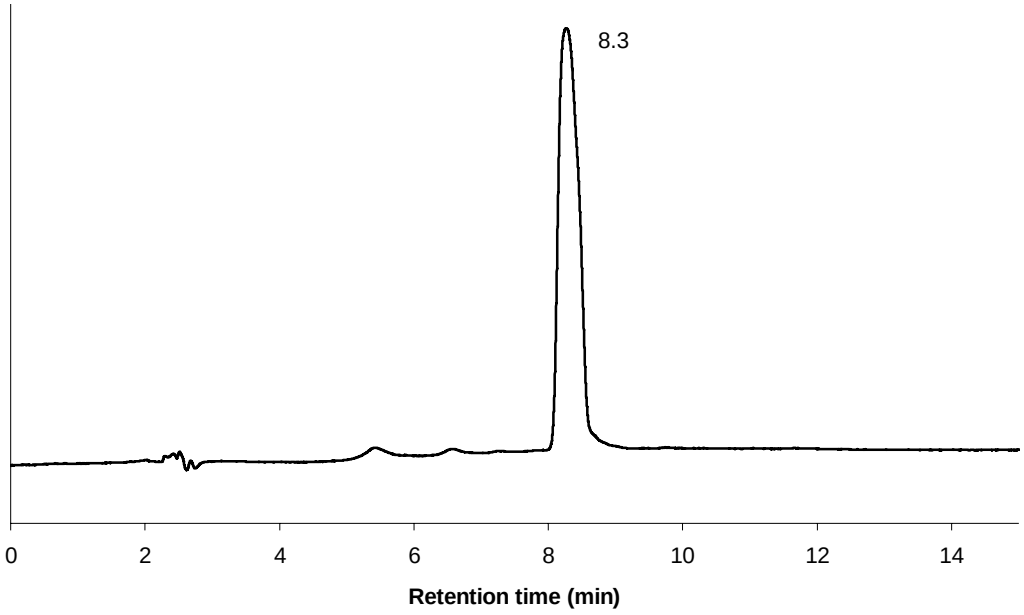

Figure S29, Chromatogram of a solution of compound **12** in MeOH. HPLC purity screening is performed on a CM4000 multiple solvent delivery system connected to a SpectroMonitor 3100 UV-Vis detector (LDC/Milton Roy) using a LiChrospher 100 RP-18 (5 μm) endcapped column (250 × 4.6 mm). The flow rate is 1.0 mL/min and the detector wavelength is set to 490 nm. Mobile phase (gradient): 70/30 MeOH/H_2O to 100/0 % MeOH/H_2O in 5 min.

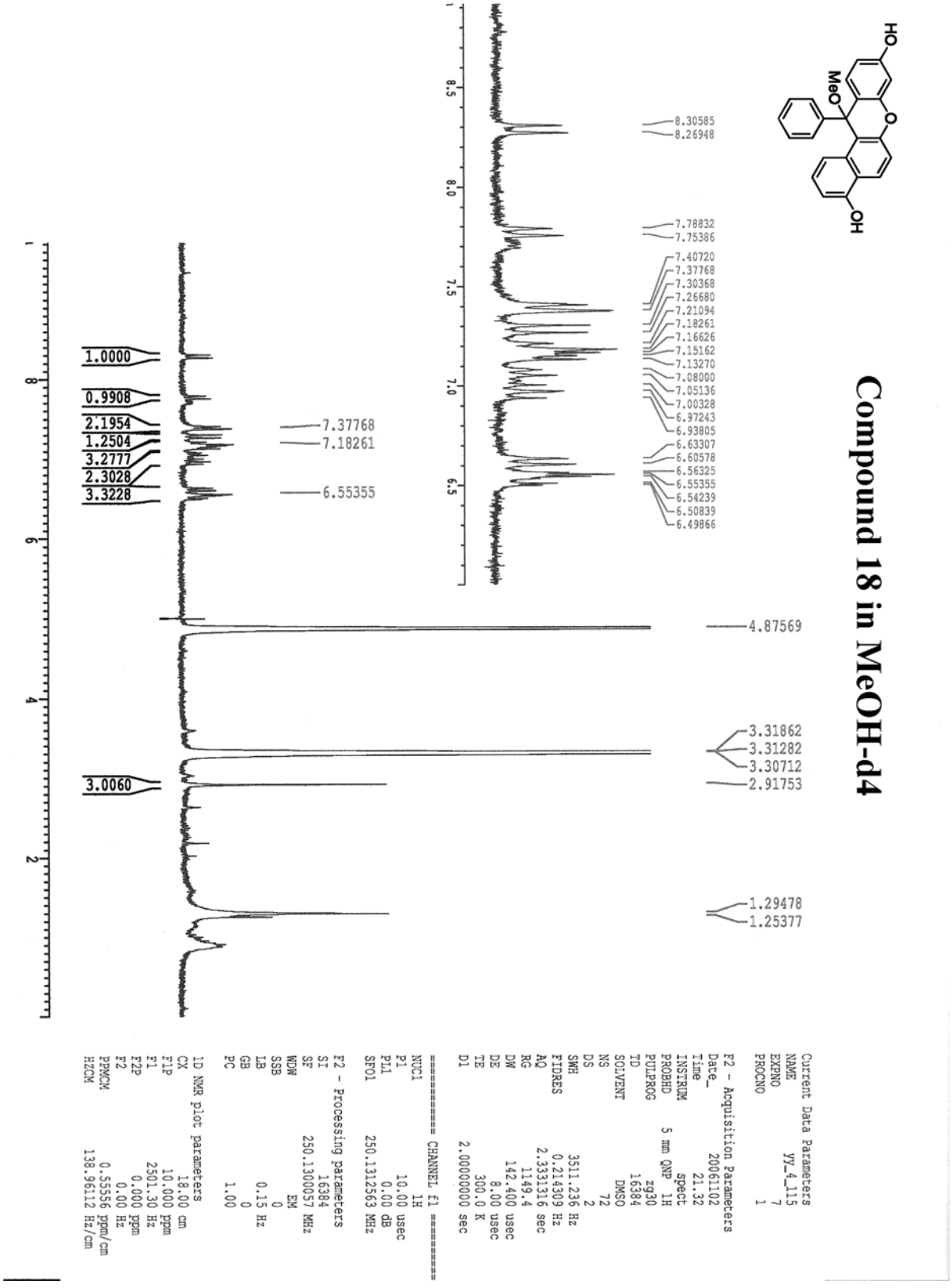

Figure S30: ^{1}H NMR of compound **18** MeOH-d_4

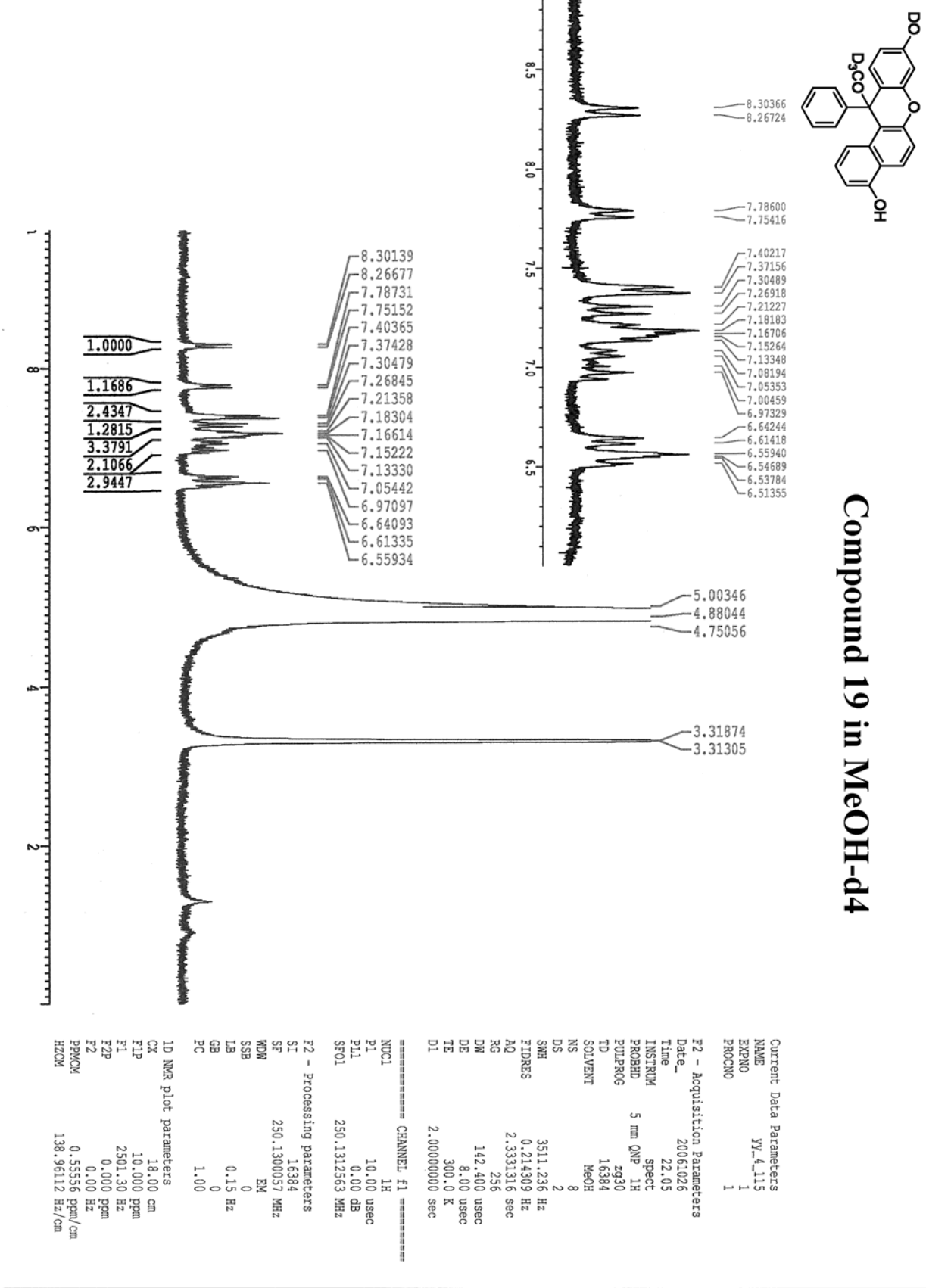

Figure S31: ^{1}H NMR of compound **19** MeOH-d_4

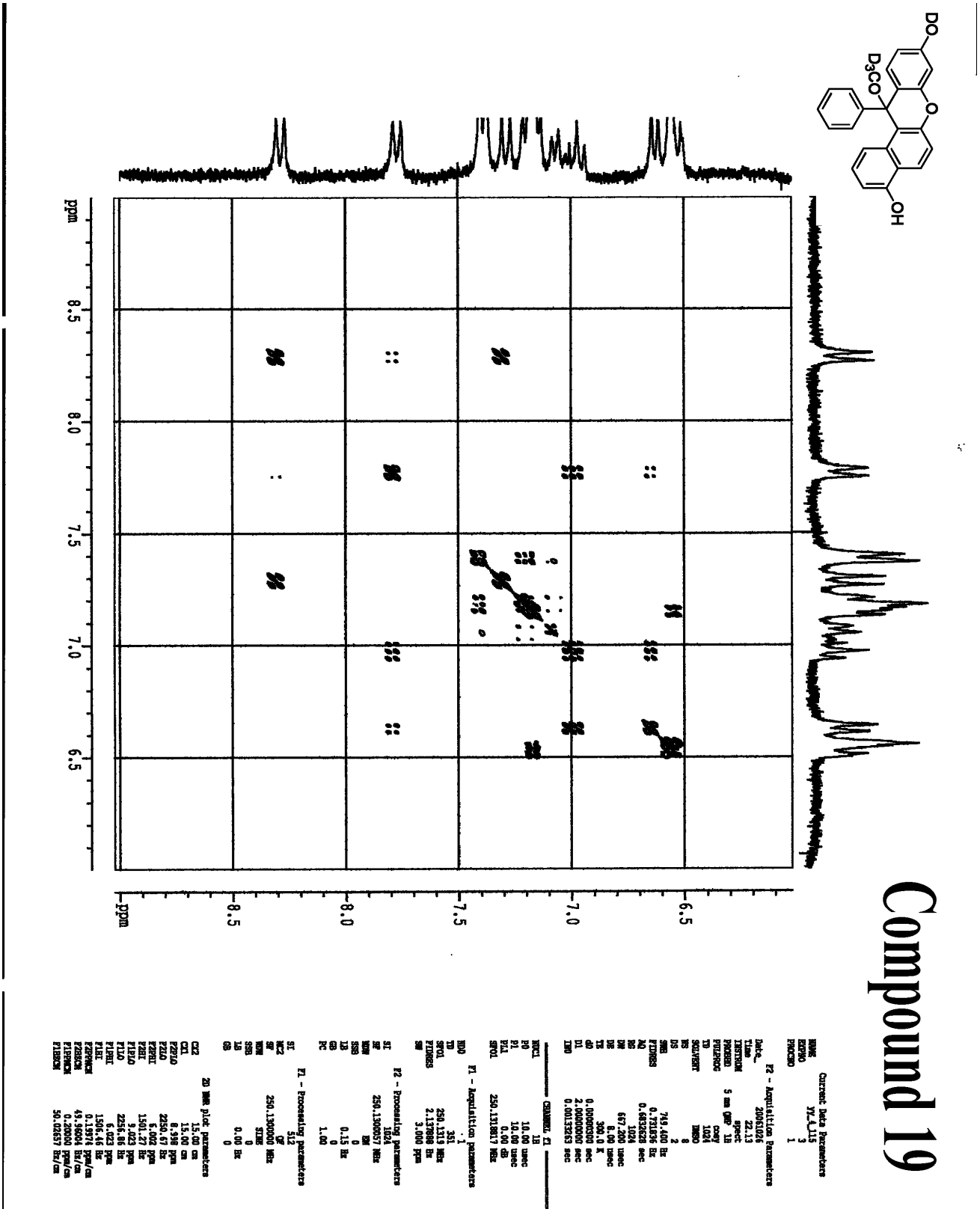

Figure S32: 2D-COSY of compound **19** (expansion from 6.0-9.0 ppm) in DMSO-d_6 Compound **18** has the same 2D-COSY spectrum shown above (expansion from 6.0 ppm to 9.0 ppm).

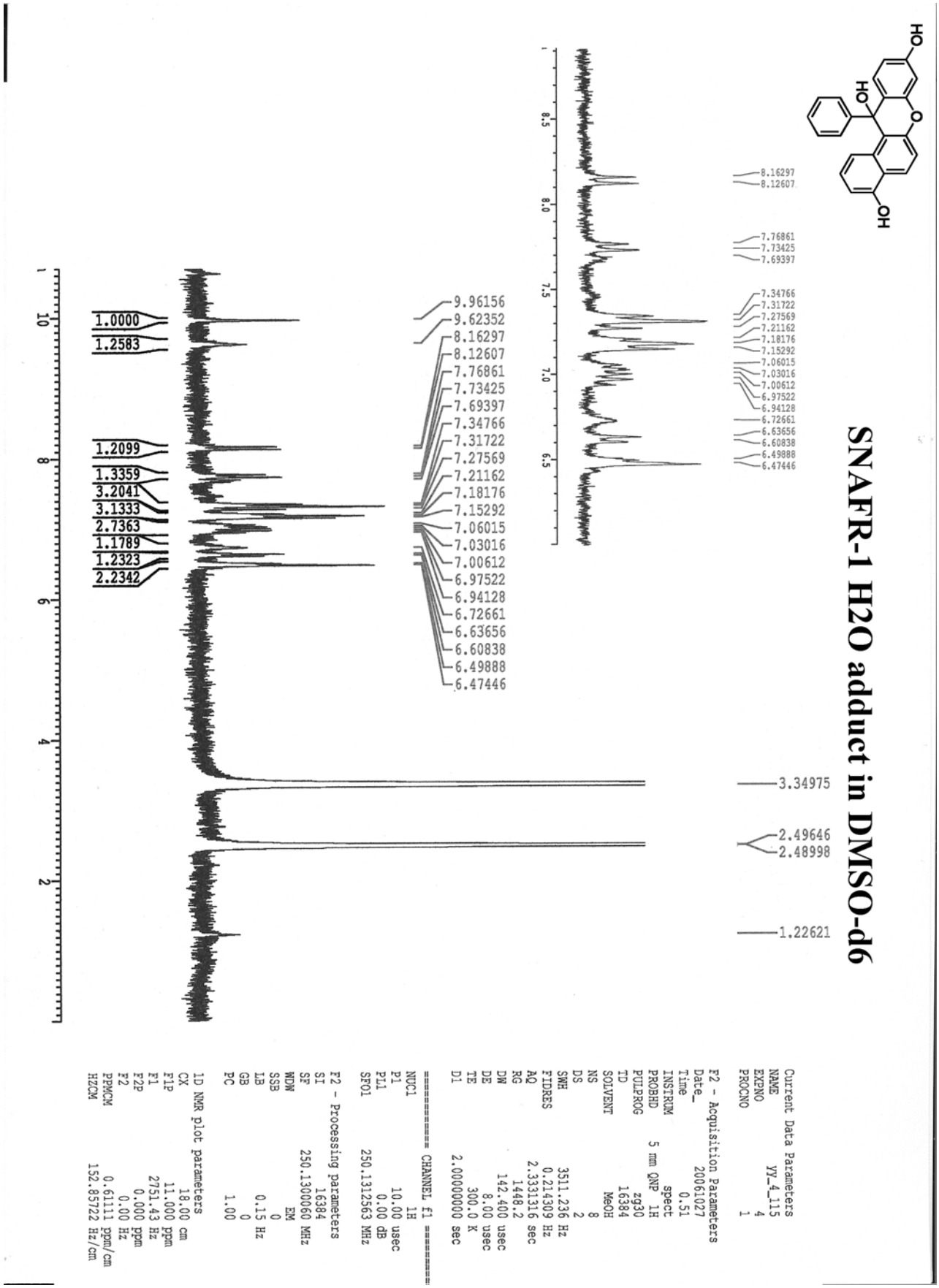

Figure S33: ^{1}H NMR of **SNAFR-1** H_2O adduct (tentatively) in DMSO-d_6.

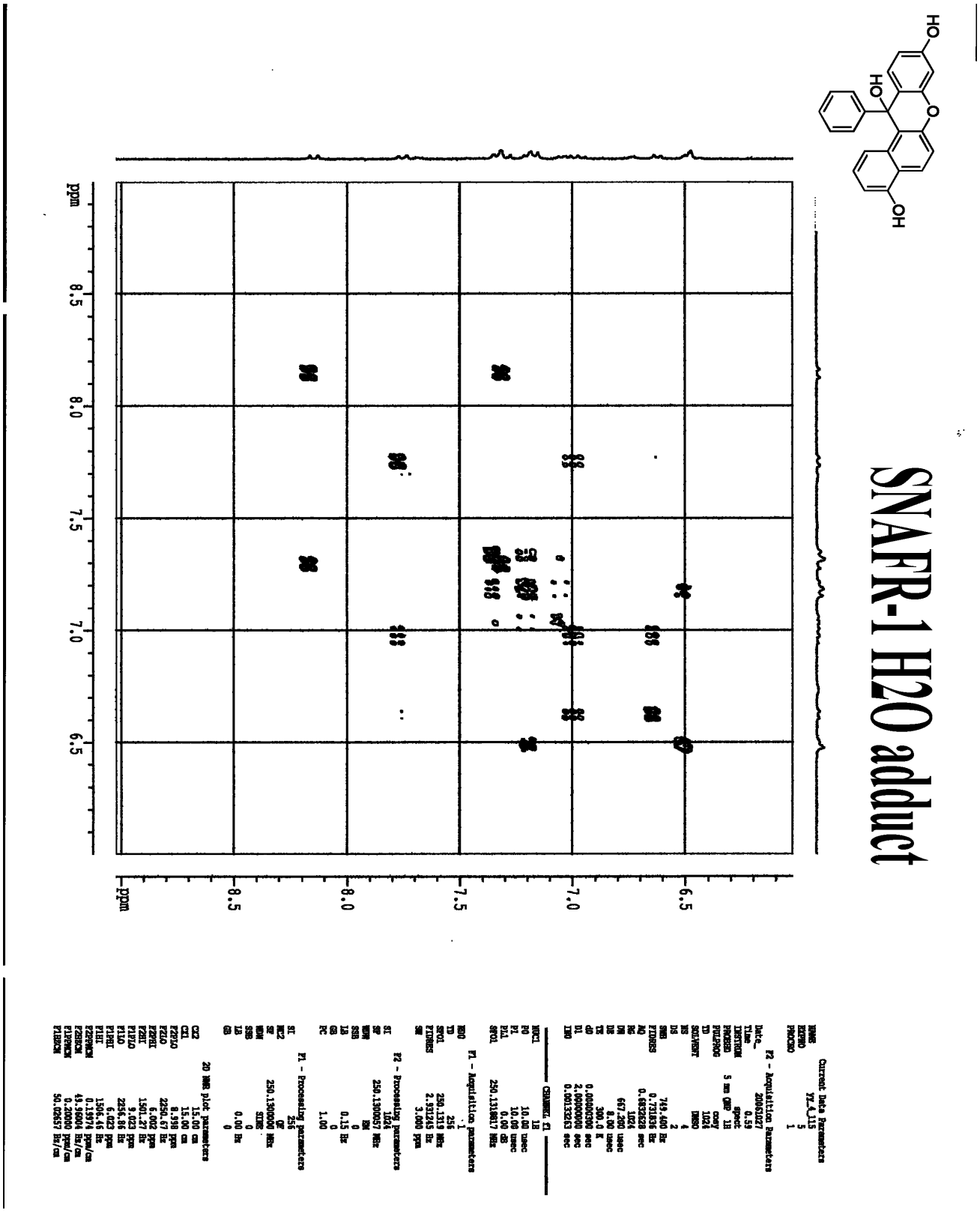

Figure S34: 2D-COSY of **SNAFR-1** H_2O adduct (tentatively) (expansion from 6.0-9.0 ppm) in DMSO-d_6.

Table S1: Assignment of protons of compound **17** based 2D COSY (Figure S14, page S15).

Compound **17**, Page S13	# of H	ppm	J (Hz)	Splitting
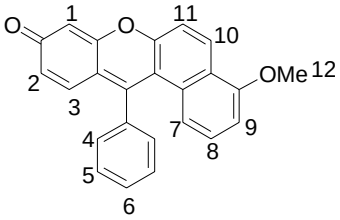	1	6.32	2.3	d
	2	6.52	9.8, 2.3	dd
	3	7.01	9.8	d
	4, 6	7.65-7.70		m
	5	7.43-7.49		m
	7	6.55	8.8	d
	8	7.11	8.8, 7.8	dd
	9	6.96	7.8	d
	10	8.58	9.5	d
	11	7.72	9.5	d
	12	3.96		s

Table S2: Assignment of protons of **SNAFR-1** based 2D COSY (Figure S19, page S20).

SNAFR-1, Page S20	# of H	ppm	J (Hz)	Splitting
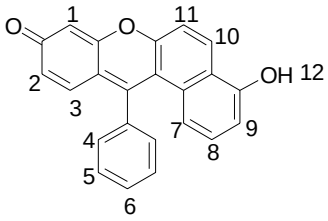	1	6.32	1.8	d
	2	6.51	9.9, 1.8	dd
	3	7.00	9.9	d
	4&6	7.64-7.69		m
	5	7.44-7.48		m
	7	6.43	8.4	d
	8	6.98	8.4,7.2	dd
	9	6.84	7.2	d
	10	8.58	9.3	d
	11	7.66	9.3	d
	12	10.57		s

Table S3: Assignment of protons of **SNAFR-2** based 2D COSY (Figure S24, page S25).

SNAFR-2, Page S23	# of H	ppm	J (Hz)	Splitting
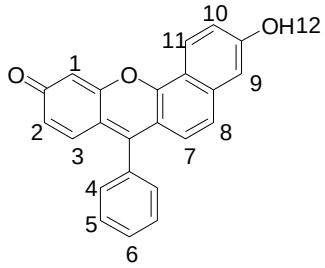	1	7.23	2.7	d
	2	7.32	9.3, 2.7	dd
	3	8.52	9.3	d
	4&6	7.65-7.70		m
	5	7.49-7.53		m
	7	7.56	9	d
	8	7.04	9	d
	9	6.50	1.5	d
	10	6.52	9.3, 1.5	dd
	11	7.09	9.3	d
	12	10.61		s

Table S4: Assignment of protons of compound **12** based 2D COSY (Figure S27, page S28).

Compound **12**, Page S28	# of H	ppm	J (Hz)	Splitting
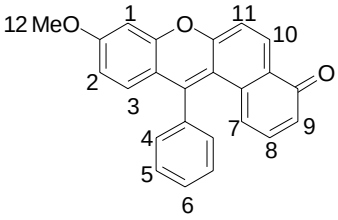	1	6.72	2.7	d
	2	6.66	9.0, 2.7	dd
	3	7.28	9	d
	4	7.36	7.2	d
	5	7.21	7.2	t
	6	7.05	7.2	t
	7	7.79	8.7	d
	8	7.01	8.7, 7.5	dd
	9	6.65	7.5	d
	10	8.18	9.0	d
	11	7.32	9	d
	12	3.75		s

Table S5: Assignment of protons of compound **19** based 2D COSY (Figure S32, page S33).

Compound **19**, Page S32	# of H	ppm	J (Hz)	Splitting
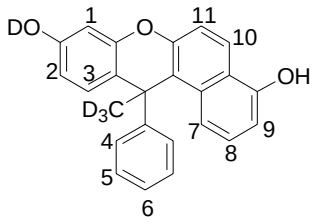	1	6.56	3.5	d
	2	6.52	3.5, 8.3	dd
	3	7.15	8.3	d
	4	7.39	7.3	d
	5	7.18	7.0	t
	6	7.05	6.5	t
	7	7.77	8.8	d
	8	6.97	8.8, 8.3	dd
	9	6.63	8.3	d
	10	8.29	9.0	d
	11	7.29	9.0	d

Table S6: Assignment of protons of **SNAFR-1** H_2O adduct based 2D COSY (Figure S34, page S35).

SNAFR-1 H_2O adduct, Page S34	# of H	ppm	J (Hz)	Splitting
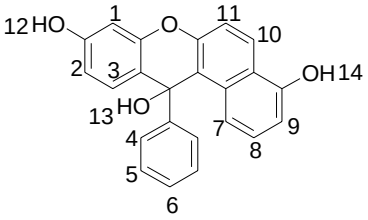	1	6.51		s
	2	6.48	9.3	d
	3	7.17	9.3	d
	4	7.34	8.5	d
	5	7.19	8.0	t
	6	7.03	6.8	t
	7	7.76	8.3	d
	8	6.98	8.3, 7.0	dd
	9	6.62	7	d
	10	8.15	9.0	d
	11	7.29	9	d
	12	9.62		s
	13	6.74		s
	14	9.96		s